eLife

Reviewed Preprint
v1 • June 30, 2025
Not revised

Microbiology and Infectious Disease

RBMX2: A Pivotal Regulator Linking *Mycobacterium bovis* Infection to Epithelial-Mesenchymal Transition and Lung Cancer Progression

Chao Wang, Yongchong Peng, Hongxin Yang, Yanzhu Jiang, Abdul Karim Khalid, Kailun Zhang, Shengsong Xie, Luiz Bermudez, Yong Yang, Lei Zhang, Huanchun Chen, Aizhen Guo, Yingyu Chen

The National Key Laboratory of Agricultural Microbiology, College of Veterinary Medicine, Huazhong Agricultural University, Wuhan, China • National Animal Tuberculosis Para-Reference Laboratory (Wuhan) of Ministry of Agriculture and Rural Affairs, Huazhong Agricultural University, Wuhan, China • Center for Infectious Disease Research, School of Medicine, Westlake University, Hangzhou, China • Oncology Collaborative Innovation Center, Inner Mongolia Medical University, Hohhot, China • Department of Biomedical Sciences, College of Veterinary Medicine, Oregon State University, Corvallis, United States • Department of Surgical Oncology, People's Hospital of Inner Mongolia Autonomous Region, Hohhot, China • Hubei Hongshan Laboratory, Huazhong Agricultural University, Wuhan, China

eLife Assessment

The study presents a comprehensive multi-approach and functional investigation of RBMX2 as a host factor involved in Mycobacterium bovis pathogenesis and its potential role in promoting epithelial-mesenchymal transition and lung cancer progression. The findings are **valuable** since the possible connection between *M. bovis* and lung cancer and the underlying mechanisms provides a promising direction for future research. The evidence is **solid** with methods, data, and analyses broadly supporting the claims, albeit with minor weaknesses that, if addressed, will make the evidence stronger. The study remains of great interest to microbiology, oncology, and drug discovery scientists.

https://doi.org/10.7554/eLife.107132.1.sa4

Abstract

The emergence and progression of tuberculosis (TB) result from the intricate interplay among the pathogen, host, and environmental factors. In 2022, there were 10.6 million new TB cases reported globally, leading to 1.3 million deaths. In regions with a high prevalence of zoonotic TB, *Mycobacterium bovis* (*M. bovis*) accounts for approximately 10% of human TB cases. The immune evasion mechanisms and latent infections of *Mycobacterium tuberculosis* (*M. tb*) complicate our understanding of the host immune response to TB. This study identifies a novel host factor, RNA-binding motif protein X-linked 2 (RBMX2), which shows potential against *M. bovis* infection. However, the specific molecular mechanisms and roles of RBMX2 during *M. bovis* infection remain poorly understood. Our investigations revealed that

following infection, RBMX2 was highly expressed in various cell types, including embryonic bovine lung (EBL) cells, bovine macrophage (BoMac) cells, bovine lung alveolar primary cells, and human pulmonary alveolar epithelial cells (A549). Using a multifaceted approach that included global transcriptional sequencing, proteomics, cell adhesion assays, ChIP-PCR, and Western blot analyses, we demonstrated that RBMX2 inhibits cell adhesion and tight junction formation in EBL cells while promoting the adhesion and invasion of *M. bovis* through the activation of the p65 pathway. Furthermore, our data suggest that RBMX2 regulates epithelial-mesenchymal transition (EMT), a process strongly associated with cancer, as indicated by our global transcriptomics, proteomics, and metabolomics analyses. To further explore the relationship between RBMX2 and cancer, we analyzed the TIMER2.0 database and found elevated expression levels of RBMX2 in lung adenocarcinoma (LUAD) and lung squamous carcinoma (LUSC) tissues compared to normal lung tissues. This finding was corroborated by immunofluorescence validation. After constructing an *M. bovis*-infected BoMac-induced EBL-EMT model, we confirmed that RBMX2 contributes to EMT by activating the p65/MMP-9 pathway post-infection.

This study elucidates the role of *RBMX2* as a novel host factor with potential anti-TB functions that inhibit TB-induced EMT. These insights have vital implications for the development of TB vaccines and therapeutic strategies for TB-mediated lung cancer, highlighting *RBMX2* as a promising target for future research.

Introduction

Tuberculosis (TB) remains a significant global health challenge, with approximately 10.6 million new cases reported in 2022, leading to 1.3 million deaths worldwide [1]. *Mycobacterium tuberculosis* (*M. tb*) variant *Mycobacterium bovis* (*M. bovis*), a zoonotic pathogen, accounts for approximately 10% of human TB cases in regions with high prevalence of zoonotic diseases. The immune evasion mechanisms employed by *M. tb* pose challenges in understanding the host immune response and the progression of TB.

Recent studies have highlighted the interplay between chronic infections, such as TB, and cancer development [2], [3]. Emerging evidence suggests that the inflammatory environment induced by persistent infections can contribute to cellular transformations associated with epithelial-mesenchymal transition (EMT), a process linked to cancer metastasis [4]. However, the specific mechanisms underlying this relationship, particularly concerning host factors involved in TB infection, remain poorly understood.

In this context, we focus on RNA-binding motif protein X-linked 2 (RBMX2), a host factor that has emerged as a potential modulator of both TB infection and cancer progression. In previous studies, we also reported that RBMX2 can regulate the retention of APAF-1 introns through alternative splicing, mediating apoptosis following *M. bovis* infection [5]. Moreover, previous research also indicates that RBMX displays significant and contrasting effects depending on the tumor type, functioning either as an oncogene or a tumor suppressor. For instance, its overexpression has been associated with hepatocellular carcinoma [6] and T-cell lymphomas[7], while a reduction in RBMX levels has been noted in Pancreatic ductal adenocarcinoma[8], suggesting a role in tumorigenesis and metastasis. However, RBMX2 involvement in TB infection and its regulatory effects on EMT have not been thoroughly investigated.

This study aims to elucidate the role of RBMX2 in *M. bovis* infection and its impact on EMT in epithelial cells. We hypothesize that RBMX2 promotes the adhesion and invasion of *M. bovis* in host cells while facilitating the EMT process through the activation of the p65/MMP-9 signaling pathway. By investigating these interactions, we seek to provide insights into the potential dual role of RBMX2 in TB and lung cancer, highlighting its significance as a therapeutic target.

Results

Elevated expression of RBMX2 in *Mycobacterium bovis*-infected cells and tuberculous Lesions

M. bovis was used to infect the EBL cell library that was constructed using CRISPR/Cas9 technology in our laboratory at a multiplicity of infection (MOI) of 100:1. We assessed cell survival and conducted high-throughput sequencing on the viable cells to identify key host factors with potential anti-*M. bovis* capabilities. Notably, the RBMX2 knockout cells exhibited significant resistance to the infection.

Further analysis using AlphaFold multimer revealed that amino acid positions 56–134 of *RBMX2* contain an RNA recognition sequence (**Supplementary Fig. 1A**). Additionally, we identified 611 RBM family sequences at the bovine protein exon level and categorized them into subfamilies based on motif similarity. *RBMX2* was primarily classified within subfamily VII, which includes proteins such as *EIF3G*, *RBM14*, *RBM42*, *RBMX44*, *RBM17*, *PUF60*, *SART3*, and *RBM25* (**Supplementary Fig. 1B**). A comparison of amino acid sequences indicated a high degree of conservation of RBMX2 across different species (**Supplementary Table 1**).

To further confirm *RBMX2* expression in EBL cells following infection with *M. bovis* and *M. bovis* Bacillus Calmette–Guerin (BCG), we collected RNA samples at 24, 48, and 72 hours post-infection (hpi). Real-time quantitative polymerase chain reaction (RT-qPCR) results demonstrated that *RBMX2* expression was significantly upregulated after both *M. bovis* and *M. bovis* BCG infections (**Figs. 1A** and **B**). Moreover, elevated *RBMX2* levels were observed in bovine lung macrophages (BoMac cells), bovine lung alveolar primary cells, and human lung epithelial cells (A549 cells) following *M. bovis* infection (**Figs. 1C-E**).

Additionally, we investigated *RBMX2* expression in clinical tissue samples from cows affected by *M. bovis*. Livers and lung samples with visible tuberculous lesions were obtained from a slaughterhouse. RT-qPCR analysis revealed that *RBMX2* expression was upregulated in both the lungs and livers infected with *M. bovis* (**Fig. 1F**).

RBMX2 did not affect cell proliferation but inhibited epithelial cell survival during *M. bovis* infection

In generating *RBMX2* monoclonal knockout (KO) cells, monoclonal cells were selected through limited dilution in 96-well plates. Sanger sequencing was conducted to identify different monoclonal cells with distinct knockout sites (**Supplementary Fig. 2A**).

The impact of *RBMX2* knockout on EBL cells indicated that *RBMX2* did not alter cell morphology, as evidenced by cytoskeleton staining using phalloidine (**Supplementary Fig. 2B**). Additionally, cellular proliferation was assessed using the EDU assay (**Figs. 1G and H**) and CCK-8 assay (**Fig. 1I**), along with cell cycle progression evaluated by Flow cytometry (**Supplementary Fig. 2C**).

To investigate the potential role of *RBMX2* in resistance to *M. bovis* infection, we assessed the survival rate of EBL cells and H1299 cells at different hours post-infection using CCK-8 assay. The findings revealed an enhanced survival rate in both *RBMX2* knockout polyclonal and monoclonal EBL cells following *M. bovis* infection (**Figs. 1J and K**). Furthermore, RBMX2-silenced H1299 cells exhibited a higher survival rate compared to H1299 ShNc cells after *M. bovis* infection (**Fig. 1L**). Notably, *RBMX2* knockout in EBL cells and silencing in H1299 cells demonstrated significant improvements in cells survival at 96 and 120 hpi compared to Wild Type (WT) EBL cells and H1299 ShNC cells, as evidenced by crystal violet staining (**Supplementary Fig. 2D**).

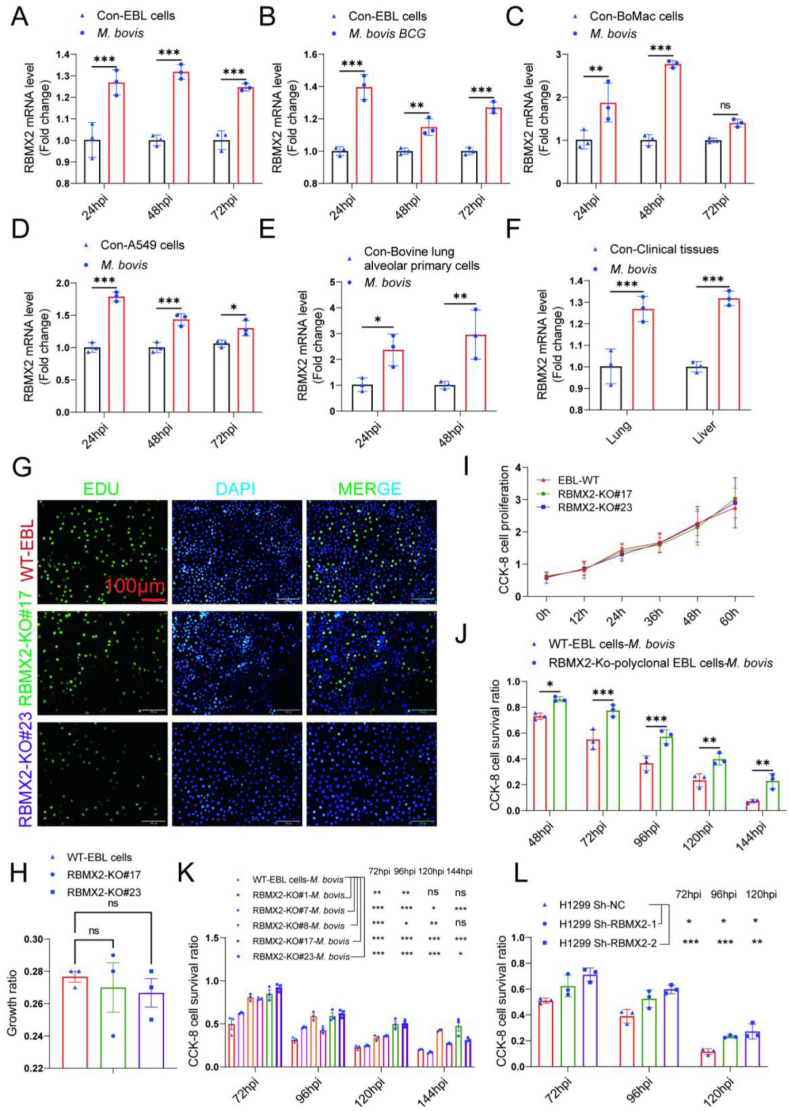

Figure 1

Expression of *RBMX2* after infection, and *RBMX2* did not affect cell proliferation but inhibited cell survival during *M. bovis* infection.

(A, B) The expression of *RBMX2* in EBL cells infected by (A) *M. bovis* and (B) *M. bovis* BCG were analyzed by RT-qPCR. Data were represented by fold expression relative to uninfected cells. (C,-E) The expression of *RBMX2* mRNA in (E) BoMac cells, (F) A549 cells, and (G) bovine lung alveolar primary cells infected by *M. bovis* were analyzed via RT-qPCR. Data were represented by fold expression relative to uninfected cells. (F) The expression of *RBMX2* mRNA in clinical TB tissues infected by *M. bovis* via RT-qPCR. Data were represented by fold expression relative to uninfected tissues. (G, H) The effect of *RBMX2* on the proliferation of EBL cells was observed by EDU assay. Data were represented by the Fluorescence cells relative to WT EBL cells. (I) The effect of *RBMX2* on the proliferation of EBL cells was observed by CCK-8 assay. Data were represented by the absorbance value relative to WT EBL cells. (J) Detection of the ability of *RBMX2* knockout Polyclonal EBL cells resisting to *M. bovis* infection by CCK-8 assay. Data were represented by the absorbance value relative to WT EBL cells after *M. bovis* infection. (K) Detection of the ability of different *RBMX2* knockout site Monoclonal EBL cells against *M. bovis* infection by CCK-8 assay. Data were represented by the absorbance value relative to WT EBL cells after *M. bovis* infection. (L) Detection of the ability of *RBMX2* slicing H1299 cells against *M. bovis* infection by CCK-8 assay. Data were represented by the absorbance value relative to Sh-NC H1299 cells after *M. bovis* infection. One-way ANOVA and two-way ANOVA were used to determine the statistical significance of differences between different groups. Ns presents no significance, * presents $p < 0.05$, **presents $p < 0.01$, and *** presents $p < 0.001$ indicate statistically significant differences. Data were representative of at least three independent experiments.

RBMX2-regulated genes associated with cell tight junction and EMT-related pathways

In investigate the role of *RBMX2* knockout in the process of *M. bovis* infection, we selected *RBMX2* knockout EBL cells and WT EBL cells at 0 (2 hpi, recorded as 0 hpi), 24, and 48 hpi for RNA-Seq analysis. A total of 16,079 genes were detected, with a significance level of $p < 0.05$ and log2 (fold change) > 2 compared to WT EBL cells. Notably, 42 genes are significantly regulated at all three-time points (0, 24, and 48 hpi) (**Fig. 2A**). Among these, 11 genes were significantly upregulated, while 31 genes were significantly downregulated. A heat map illustrates the expression level of each gene across various samples, with each row representing a specific gene and each column representing the expression levels in a given sample (**Fig. 2A**).

The functional significance of these differentially expressed genes (DEGs) in EBL cells infected with *RBMX2* knockout was further explored using GO and KEGG analyses. The most significantly affected biological processes included epithelial cell differentiation, cell adhesion and biological adhesion. The cellular components most affected were the extracellular region, extracellular region part, extracellular space, and plasma membrane part. The molecular functions primarily associated with activin receptor activity, type I (**Fig. 2B**).

The KEGG pathway entries revealed that these genes were linked to a various pathways, including ECM–receptor interaction, cGMP-PKG signaling pathway, PI3K-Akt signaling pathway, cytokine-cytokine receptor interaction, and vascular smooth muscle contraction (**Fig. 2C**). Proteomics also validated these phenotypes related to cell tight junction and EMT using 48hpi protein samples, highlighting pathways such as extracellular space, integrin binding, basement membrane, and glucose homeostasis via GO analysis, along with cell adhesion molecules, ECM-receptor interaction, and TGF-beta signaling pathway through KEGG analysis (**Figs. 2D and E**).

We also examined the impact of varying infection durations on *RBMX2* knockout EBL cellular lines via GO analysis. At 0 hpi, genes were primarily related to the pathways of cell junctions, extracellular regions, and cell junction organization (**Supplementary Fig. 3A**). At 24 hpi, genes were mainly associated with pathways of the basement membrane, cell adhesion, integrin binding and cell migration (**Supplementary Fig. 3B**). By 48 hpi, genes were annotated into epithelial cell differentiation and were negatively regulated during epithelial cell proliferation (**Supplementary Fig. 3C**). This indicated that *RBMX2* can regulate cellular connectivity throughout the stages of *M. bovis* infection.

For KEGG analysis, genes linked to the *MAPK* signaling pathway, chemical carcinogen-DNA adducts, and chemical carcinogen–receptor activation were observed at 0 hpi (**Supplementary Fig. 3D**). At 24 hpi, significant enrichment was found in the ECM–receptor interaction, PI3K–Akt signaling pathway, and focal adhesion (**Supplementary Fig. 3E**). Upon enrichment analysis at 48 hpi, significant enrichment was noted in the TGF-beta signaling pathway, transcriptional misregulation in cancer, microRNAs in cancer, small cell lung cancer, and p53 signaling pathway (**Supplementary Fig. 3F**).

To validate the RNA-seq data, we confirmed a random selection of 10 genes using RT-qPCR (**Fig. 2F**). The mRNA levels of the selected genes were consistent with the RNA-seq outcomes, including *FRMD4B*, *MCTP1*, *HSPB8*, *ST14*, and *OMD*, which are linked to scaffold proteins, cell adhesion, and epithelial barriers. Additionally, *MCTP1*, *HSPB8*, *IL-24*, *1L-7*, *GPX2*, and *NOS3* were associated with apoptosis, inflammation, and oxidative stress.

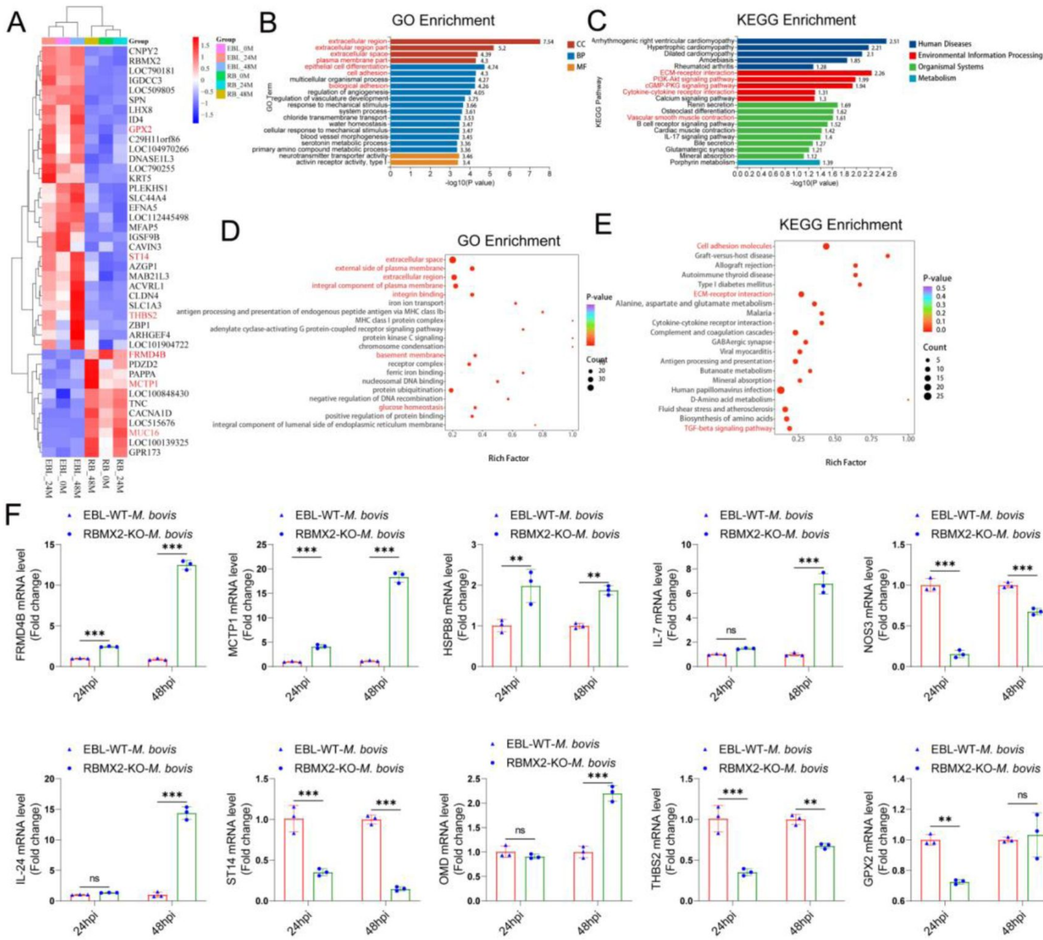

Figure 2

Transcriptome and proteomic analysis in *RBMX2* knockout and WT EBL cells after *M. bovis* infection.

(A) The heat map illustrates some genes that had been all enriched in RBMX2 knockout and WT EBL cells after *M. bovis* infection in 0, 24, and 48hpi. Red represents upregulated genes, and blue represents downregulated genes. Each group represented three independent samples. (B) GO Analysis of all enriched genes in 0, 24 and 48hpi. Data were represented as all enriched pathways in RBMX2 knockout EBL cells relative to WT EBL cells after *M. bovis* infection thrice. (C) KEGG Analysis of all enriched genes in 0, 24, and 48hpi. Data were represented as all enriched pathways in RBMX2 knockout EBL cells relative to WT EBL cells after *M. bovis* infection in three times. (D) GO Analysis of all enriched proteins in 48hpi. Data were represented as all enriched pathways in RBMX2 knockout EBL cells relative to WT EBL cells after *M. bovis* infection. (E) KEGG Analysis of all enriched genes in 48hpi. Data were represented as all enriched pathways in RBMX2 knockout EBL cells relative to WT EBL cells after *M. bovis*-infection (MOI 20) in three times. (F) Identification the expression of related genes mRNA enriched by RT-qPCR. Data were represented as the fold expression in RBMX2 knockout EBL cells relative to WT EBL cells after *M. bovis* infection. Two-way ANOVA was used to determine the statistical significance of differences between different groups. Ns presents no significance, * presents $p < 0.05$, **presents $p < 0.01$, and *** presents $p < 0.001$ indicate statistically significant differences.

RBMX2 interferes with the integrity of tight junctions in epithelial cells caused by *M. bovis*

Through transcriptome sequencing, we identified 41 genes that underwent transcript changes following *M. bovis* infection. Of these, 22 genes were upregulated, while 19 genes were downregulated (**Supplementary Figs. 4A** and **B**). The downregulated genes were primarily associated with tight junction and leukocyte transendothelial migration (**Fig. 3A**). In contrast, the upregulated genes were mainly linked to immunity-related pathways, including the defense response to viruses and regulation of viral processes (**Fig. 3B**).

Based on these finding,we hypothesized that *RBMX2* could damage the integrity of epithelial cell tight junction. To validate this prediction, we constructed a model of *M. bovis*-destroyed tight junctions in EBL cells. EBL cells were infected with *M. bovis* and we subsequently performed RT-qPCR and Western blot (WB) analyses to assess the expression of cell tight junction-related mRNAs (*TJP1*, *OCLN*, *CLDN-5*, and *CLDN-7*) and proteins (ZO-1, OCLN, and CLDN-5). We found that the expression levels of all mRNAs and proteins was significantly reduced following *M. bovis* infection compared to the uninfected coutrol (**Figs. 3C and D**).

Tight junctions are critical intercellular adhesion structures that define the permeability of barrier-forming epithelial cells [9]. The ability of epithelial cells to maintain functional intercellular adhesion is essential for forming a tight epithelial protective barrier [10]. To further investigate the effect of *M. bovis* on epithelial cell adhesion, we conducted a cell adhesion assay, revealing a significant decrease in the intercellular adhesion ratio (**Fig. 3E**). These results validated that *M. bovis* can compromise the tight junction of EBL cells.

To explore the impact of *RBMX2* on the epithelial cells barrier, we infected RBMX2 knockout and WT EBL cells with *M. bovis* and assessed the expression of epithelial barrier-related mRNAs (*TJP1*, *OCLN*, and *CLDN-5*) and proteins (ZO-1, OCLN, and CLDN-5) using RT-qPCR and WB. The *RBMX2* knockout EBL cells exhibited a significant upregulation of all three proteins compared to WT EBL cells (**Figs. 3F and G**). The cell adhesion assay also demonstrated that *RBMX2* knockout EBL cells displayed a heightened adhesion ratio relative to WT EBL cells (**Fig. 3H**).

Tight junctions are essential component of the epithelial barrier and can be compromised by bacteria infections, contributing to inflammation [11], [12]. To investigate whether *RBMX2* mediates intracellular inflammation by regulating the tightness of the epithelial barrier, we measured the mRNA levels of inflammatory factors (IL-1β, TNF, and IL-6) in *RBMX2* knockout EBL cells post-infection. The results showed a decrease in the expression of these inflammatory factors in RBMX2 knockout EBL cells compared to WT EBL cells after *M. bovis* infection (**Fig. 3I**).

In summary, our findings indicate that *RBMX2* affects the integrity of epithelial cell tight junctions, and knocking out *RBMX2* enhances tight junction formation while decreasing the inflammatory response induced by *M. bovis*.

RBMX2 disrupted the epithelial barrier via activating *p65*

The MAPK pathway and NF-kappaB pathway play crucial roles in regulating tight junctions between epithelial cells [13]-[16]. To further elucidate the regulatory mechanism of *RBMX2* in the epithelial barrier's tight junctions, we found that the MAPK pathway was enriched in our transcriptome sequencing data, and the potential regulatory transcription factor p65 was predicted through the JASPAR database (Supplementary Table 2).

We assessed the phosphorylation levels of MAPK pathway proteins and p65 protein in RBMX2 knockout EBL cells, revealing that the phosphorylation of p65 and MAPK/p38/JNK was significantly reduced in these cells after *M. bovis* infection compared to WT EBL cells (**Figs. 4A and B**).

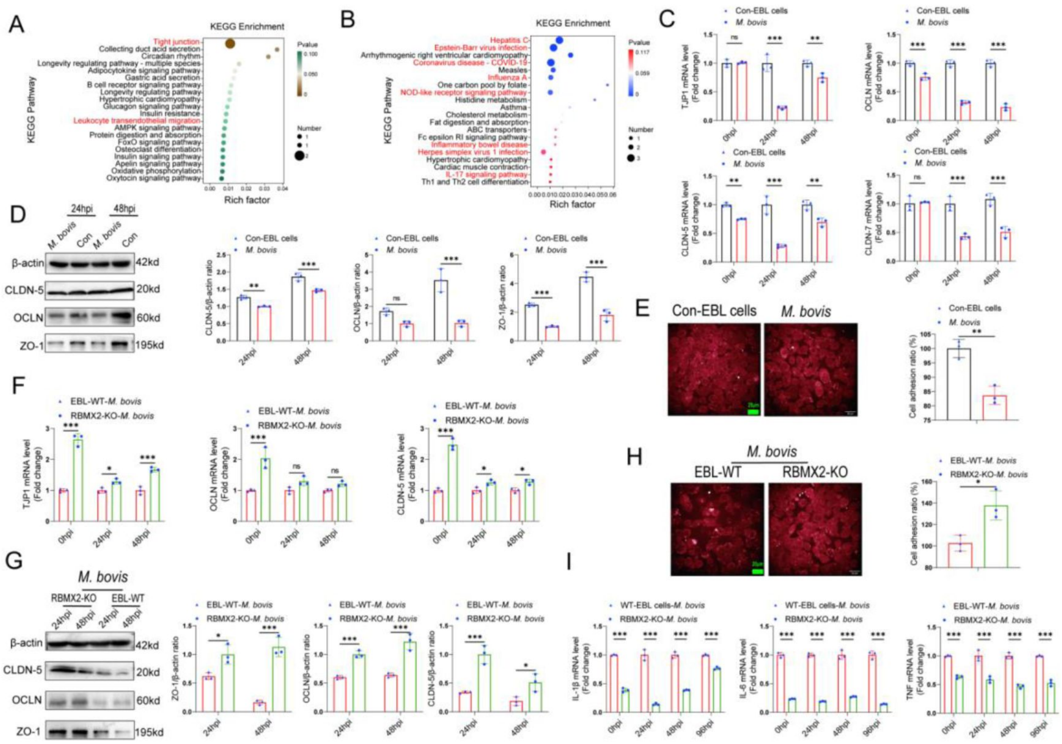

Figure 3

RBMX2 **had the potential to induce the disruption of tight junctions in EBL cells after** ***M. bovis*** **infection.**

(A, B) KEGG analysis was conducted to identify the (A) down-regulated and (B) up-regulated pathways among the enriched genes after *M. bovis* infection of WT EBL cells. Data were relative to WT EBL cells without *M. bovis* infection. (C, D) The expression of epithelial cells tight junction-related (C) mRNAs (*TJP1*, *CLDN-5*, *CLDN-7,* and *OCLN*) and (D) proteins (ZO-1, CLDN-5, and OCLN) were assessed after *M. bovis* infection of WT EBL cells via RT-qPCR and WB. Data were relative to WT EBL cells without *M. bovis* infection. (E) Cell adhesion ratio was evaluated via cell adhesion assay after WT EBL cells were infected with *M. bovis* using High-content imaging. Data were relative to WT EBL cells without *M. bovis* infection. Scale bar: 20 μm. (F, G) The expression of epithelial tight junction-related (F) mRNAs (*TJP1*, *CLDN-5*, and *OCLN*) and (G) proteins (ZO-1, CLDN-5, and OCLN) in *RBMX2* knockout EBL cells after *M. bovis*-infection through RT-qPCR and WB. Data were relative to WT EBL cells with *M. bovis* infection. (H) Cell adhesion assay was conducted to assess the cell adhesion ratio of *RBMX2* knockout EBL cells after infection with *M. bovis*. Data were relative to WT EBL cells with *M. bovis* infection. Scale bar: 20 μm. (I) Expression of inflammatory factors-related factors (*IL-6*, *IL-1β*, and *TNF*) were assessed after *RBMX2* knockout EBL cells infected by *M. bovis*. Data were relative to WT EBL cells with *M. bovis* infection. T-test and Two-way ANOVA were used to determine the statistical significance of differences between different groups. Ns presents no significance, * presents $p < 0.05$, **presents $p < 0.01$, and *** presents $p < 0.001$ indicate statistically significant differences. Data were representative of at least three independent experiments.

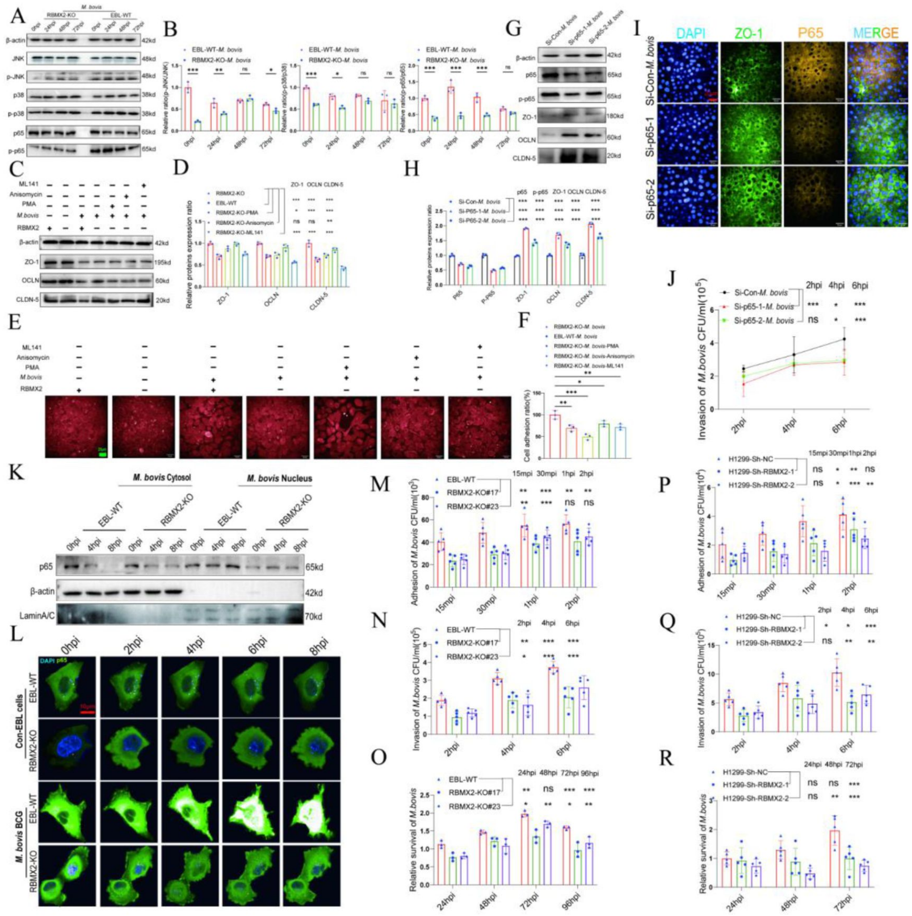

Figure 4

RBMX2 facilitated the disruption of epithelial tight junctions through the promotion of p65 protein phosphorylation and translocation and then enhanced the processes of *M. bovis* adhesion, invasion, and intracellular survival.

(A, B) Activation of the MAPK pathway-related protein and p65 protein were activated after *RBMX2* knockout and WT EBL cells infected by *M. bovis* via WB. Data were relative to WT EBL cells with *M. bovis* infection. (C, D) Expression of tight junction-related proteins (ZO-1, CLDN-5, and OCLN) was assessed in *RBMX2* knockout EBL cells treated with three p38/p65/JNK pathways activators after *M. bovis* infection via WB. Data were relative to *RBMX2* knockout EBL cells untreated activators with *M. bovis* infection. (E, F) Evaluate the impact of three *p38/p65/JNK* pathways activators on the ratio of intercellular adhesion via cell adhesion assay. Data were relative to *RBMX2* knockout EBL cells untreated activators with *M. bovis* infection. Scale bar: 20 μm. (G, H) Evaluate the silencing efficiency of siRNA on p65 protein expression and its impact on the expression of ZO-1, CLDN-5, and OCLN proteins through WB. Data were relative to SiRNA-NC in WT EBL cells with *M. bovis* infection. (I) Detect the correlation between p65 expression and ZO-1 in WT EBL cells after *M. bovis* infection via IF analysis. ZO-1 is stained with green fluorescence, p65 is stained with yellow fluorescence, and the nucleus is stained with blue fluorescence. Data were relative to SiRNA-NC in WT EBL cells with *M. bovis* infection. (J) The effect of p65 silencing on the invasive ability of *M. bovis* in WT EBL cells. Data were relative to SiRNA-NC in WT EBL cells with *M. bovis* infection. (K) The effect of *RBMX2* on the nuclear translocation of p65 protein after *M. bovis* infection using WB. β-actin presents cytosol and Lamin A/C presents nucleus. Data were relative to RBMX2 knockout EBL cells after *M. bovis* infection. (L) The effect of *RBMX2* on the nuclear translocation of p65 protein after *BCG*-infection using High-content real-time imaging. Using pCMV-EGFP-p65 plasmid transfect RBMX2 knockout and WT EBL cells. The nucleus is stained with blue fluorescence. Data were relative to WT EBL cells without BCG infection. (M, N, O) The impact of *M. bovis* on the adhesion, invasion, and intracellular survival of *RBMX2* knockout and WT EBL cells through plate counting. Data were relative to WT EBL cells after *M. bovis* infection. (P, Q, R) The impact of *M. bovis* on the adhesion, invasion, and intracellular survival of Sh-NC and Sh-RBMX2 H1299 cells through plate counting. Data were relative to H1299 ShNC cells after *M. bovis* infection. One-way ANOVA and two-way ANOVA were used to determine the statistical significance of differences between different groups. Ns presents no significance, * presents $p < 0.05$, **presents $p < 0.01$, and *** presents $p < 0.001$ indicate statistically significant differences. Data were representative of at least three independent experiments.

To determine whether RBMX2 specifically regulates the MAPK/p38/JNK proteins and p65 to promote tight junction disruption and decrease intercellular adhesion, *RBMX2* knockout EBL cells were treated with *PMA* (*p65* activator), *Anisomycin* (*JNK* activator), and *ML141* (*p38* activator) for 12 h prior to *M. bovis* infection. The optimal concentrations for these activators were determined through WB and CCK-8 cell viability assays, yielding 100 nm for PMA, 10 µm for *Anisomysin*, and 10 µm for ML141, all without significant effects on cell viability (**Supplementary Figs. 5A, B**, and **C**). WB results indicated that the p65 and *MAPK/p38* pathways could impede the expression of tight junction proteins (ZO-1, OCLN, and CLDN-5) following *M. bovis* infection (**Figs. 4C and D**).

To examine whether RBMX2 regulates cell adhesion ratio via p65 and MAPK/p38/JNK pathways, we investigated the impact of *p65*, *p38* and *JNK* activators on cell adhesion in *RBMX2* knockout EBL cells. Cell adhesion assays showed that treatment with p65 activator significantly reduced cell adhesion ratio compared to the p38 and JNK activators (**Figs. 4E and F**).

To further substantiating the association between p65 and tight junction regulation in WT EBL cells after *M. bovis* infection, we used siRNA to inhibit p65. WB analysis demonstrated that siRNA significantly reduced p65 and *p-p65* expression (**Figs. 4G and H**). WB and Immunofluorescence (IF) analyses revealed that suppressing p65 facilitated the expression of ZO-1, OCLN, and CLDN-5 after *M. bovis* infection (**Figs. 4G**, H and I). Additionally, silencing p65 in WT EBL cells inhibited the invasion of *M. bovis* into epithelial cells, as shown by plate counting assay (**Fig. 4J**).

Finally, to investigate the relationship between *RBMX2*-mediated p65 and the findings above, EBL cells were infected with *M. bovis* and *M. bovis* BCG. WB and high-content live imaging system outcomes demonstrated diminished nuclear translocation of the p65 protein in *RBMX2* knockout EBL cells compared with WT EBL cells (**Figs. 4K and L**).

In summary, our findings validate that *RBMX2* can regulate the phosphorylation and nuclear translocation of p65 protein, leading to the degradation of tight junction proteins in EBL cells infected with *M. bovis*.

RBMX2 promotes adhesion, invasion, and intracellular survival of pathogens

Disrupting the intercellular tight junction barrier enhances bacterial adhesion and invasion [17,18]. Based on these findings, we hypothesize that *RBMX2* may facilitates the adhesion and invasion of *M. bovis* by degrading the tight junction proteins in EBL cells. To test this hypothesis, EBL cells were infected with *M. bovis* at an MOI of 20:1, plate count assays indicated a significant reduction in *M. bovis* adhesion in *RBMX2*-KO#17 and KO#23 EBL cells compared with WT EBL cells (**Fig. 4M**) at 15 min, 30 min, 1 h, and 2 h post-infection (**Fig. 4N**). Furthermore, the invasion of *M. bovis* in *RBMX2*-KO#17 and KO#23 EBL cells was decreased at 2, 4, and 6 h post-infection compared with WT EBL cells. Additionally, the intracellular survival of *M. bovis* in *RBMX2*-KO#17 and KO#23 EBL cells was lower at 24, 48, 72 and 96 hpi compared with WT EBL cells (**Fig. 4O**). Silencing *RBMX2* in human lung epithelial cells (H1299) also led to a significant reduction in the adhesion, invasion, and intracellular survival of *M. bovis* (**Figs. 4P-R**). Thus, the host factor *RBMX2* is critical for promoting the adhesion, invasion, and intracellular survival of *M. bovis*.

In addtion, pathway activators were employed to investigate the relationship between pathway activation and the regulation of *M. bovis* adhesion and invasion by *RBMX2*. The results showed that applying a p65 activator to *RBMX2* knockout EBL cells significantly impaired the tight junction function of the epithelial barrier, thereby enhancing *M. bovis* adhesion and invasion in EBL cells by regulating the phosphorylation and nucleation of p65 (**Supplementary Figs. 6A** and **B**). Hence, RBMX2 promotes *M. bovis* adhesion and invasion in EBL cells by regulating the phosphorylation and nucleation of p65

To further explore the influence of *RBMX2* on adhesion and invasion in the context of different virulence *Mycobacterial* species, we utilized attenuated virulent *M. bovis* BCG and *Mycobacterium smegmatis* (*M. smegmatis*) to infect EBL cells. The plate count assays revealed a significant reduction in the adhesion of both *M. bovis* BCG and *M. smegmatis* in *RBMX2* knockout EBL cells at various time points post-infection compared to WT EBL cells (**Supplementary Figs. 6C** and D). Additionally, the invasion of *M. bovis* BCG and *M. smegmatis* was markedly diminished at different hpi in *RBMX2* knockout EBL cells (**Supplementary Figs. 6E** and F). Consequently, the virulence of *Mycobacterium* does not appear to affect the capacity of *RBMX2* to promote the adhesion and invasion of *M. bovis* BCG and *M. smegmatis* in EBL cells.

Furthermore, we examined the role of *RBMX2* in regulating other bacteria associated with bovine pneumonia by infecting EBL cells with *Salmonella* and *Escherichia coli* (*E. coli*). Our findings indicated that *RBMX2* knockout EBL cells exhibited a degree of inhibition in bacterial adhesion and invasion across all tested bacterial species compared to WT EBL cells (**Supplementary Figs. 6G-J**).

In summary, our experiments provide compelling evidence that RBMX2 broadly promotes the adhesion and invasion of pathogens associated with bovine pneumonia, highlighting its potential as a target for developing disease-resistant cattle.

RBMX2 is highly expressed in lung cancer and regulates cancer-related metabolites

Previous studies have demonstrated a link between bacterial infection and the initiation of EMT [19-21]. Prolonged infection with *M. tb* or *M. bovis* induces oxidative stress, activates Toll-like receptors (TLR), and elicits the release of inflammatory cytokines [22-24]. Consequently, this phenomenon creates a favorable microenvironment for tumor development, progression, and dissemination [25, 26]. Epidemiological investigations have established a correlation between TB and the occurrence of lung cancer [27-30]. However, the precise cellular mechanism underlying this association remain unclear.

In our research, we conducted a comprehensive analysis of gene families, revealing a remarkable degree of *RBMX2* conservation among bovine, monkey, and human sources (**Fig. 5A**). To further elucidate the involvement of *RBMX2* in cancer, we utilized the *TIMER2.0* database to assess its expression patterns across various cancer types within The Cancer Genome Atlas (TCGA). Our findings indicated a notable upregulation of *RBMX2* in lung cancer, specifically in lung adenocarcinoma (LUAD) and lung squamous cell carcinoma (LUSC) (**Fig. 5B**).

To investigate the elevated expression of *RBMX2* in lung cancer further, we measured its expression in both lung cancer epithelial cell lines and normal lung epithelial cell lines using RT-qPCR. The results demonstrated that *RBMX2* expression in lung cancer epithelial cell lines (NCIH1299, NCIH460, and CALU1) was significantly higher than that in normal lung epithelial cells (BEAS-2B) (**Fig. 5C**). Additionally, immunofluorescence (IF) analysis revealed that *RBMX2* expression levels were also higher in LUAD and LUSC tumor tissues compared to adjacent non-cancerous lung tissues (**Figs. 5D-F**).

Furthermore, we investigate whether *RBMX2* regulates specific EMT-related metabolites to mediate the EMT process in EBL cells following *M. bovis* infection. Our metabolomic analysis of EBL cell samples at 48 hpi revealed that *RBMX2* knockout primarily enriched pathways related to nucleotide metabolism, biosynthesis of cofactors, biosynthesis of nucleotide sugars, pentose and glucuronate interconversions, vascular smooth muscle contraction, amino sugar, and nucleotide sugar metabolism, chemokine signaling pathway, aldosterone synthesis and secretion, and cGMP-PKG signaling pathway. Thes pathways are associated with tumor cells proliferation, migration,

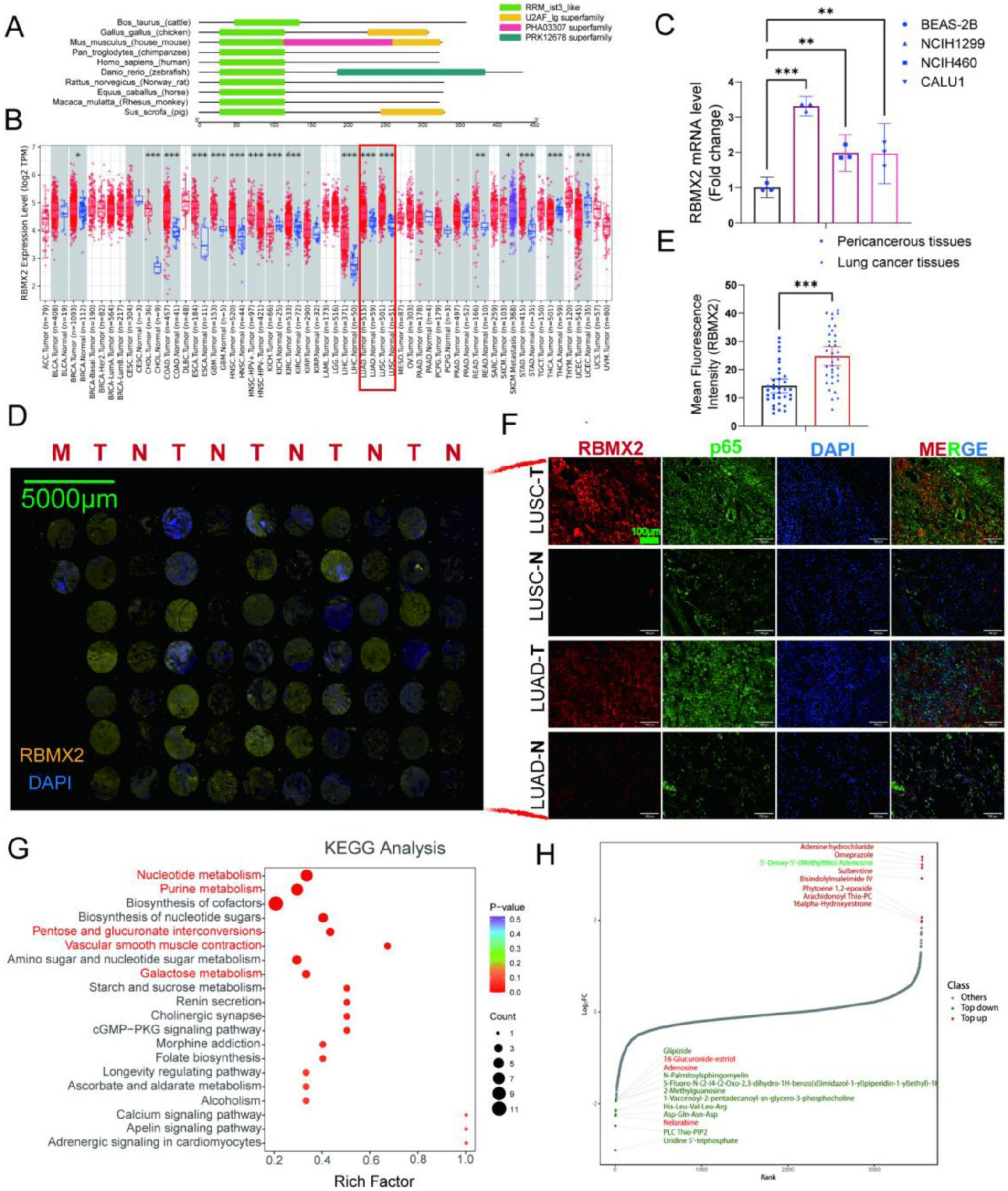

Figure 5

RBMX2 is highly expressed in tumor tissues and regulates cancer-related metabolites

(A) A comparative analysis of the functional domains of the *RBMX2* protein across ten different species. (B) Analyzing the expression patterns of *RBMX2* in pan cancer using *TIMER2.0* cancer database. (C) The expression of *RBMX2* in different lung cancer cells and normal lung epithelialcells via RT-qPCR. Data were relative to normal lung epithelialcells (BEAS-2B). (D-E) The expression of *RBMX2* in lung cancer clinical tissues via IF. RBMX2 is stained with yellow fluorescence, and the nucleus is stained with blue fluorescence. Data were relative to pericancerous lung tissues. Scale Bar: 5000 μm. (F) The expression of *RBMX2* and p65 in LUAD and LUSC clinical tissues via IF. *RBMX2* is stained with red fluorescence, p65 is stained with green fluorescence, and the nucleus is stained with blue fluorescence. Data were relative to normal lung tissues. Scale Bar: 100 μm. (G) KEGG analysis of differential metabolite enrichment pathways in *RBMX2* knockout EBL cells compared to WT EBL cells after *M. bovis* infection. (H) Dynamic distribution map of top 20 differential metabolites in RBMX2 knockout EBL cells compared to WT EBL cells after *M. bovis* infection.

and invasion (**Fig. 5G**). Differential metabolites are related to tumor metabolism, mainly including 6-glucuronic acid estriol, adenosine, uridine 5 '-triphosphate, and 5' - deoxy-5 '-(methylthio) (**Figure 5H**).

RBMX2 promotes the transformation of EBL cells from epithelial cells to mesenchymal cells

To investigate the association between *RBMX2* and EMT induced by *M. bovis*, we intially infected EBL cells directly with *M. bovis*. This infection did not effectively induce the expression of mesenchymal cell marker proteins (**Supplementary Fig. 7A**). Previous literature indicates that *M. bovis* infection in macrophages, along with its secreted proteins, can stimulate the production of cytokines such as TNF, IL-6, and TGF-β, all of which promote EMT process [31-34].

To further explore the impact of *M. bovis* infection on EMT progression in EBL cells, we constructed a coculture model using *M. bovis*-infected BoMac cells (**Fig. 6A** and **Supplementary Fig. 7B**). In this model, we identified EMT-related cytokines, including IL-6 and TNF, in *M. bovis*-infected BoMac cells, revealing a significant increase compared to uninfected BoMac and EBL cells (**Fig. 6B**). Notably, *RBMX2* expression was upregulated in EBL cells within this coculture model following *M. bovis* infection (**Fig. 6C**).

We then examined the morphology changes in epithelial cells within the coculture model using electron microscopy. The results demonstrated that most cells transitioned from circular to an elongated morphology (**Fig. 6D**). Staining of the EBL cells cytoskeleton with ghost pen cyclic peptide highlighted significant morphological alterations, with EBL cells transforming from spherical to spindle-shaped (**Supplementary Fig. 7C**).

Additionally, we assessed the expression of EMT-related mRNAs and proteins in EBL cells after coculture with *M. bovis-infected* BoMac cells. This analysis reveald a significant downregulation of the epithelial cell marker protein *E-cadherin* and a notable upregulation of mesenchymal markers *N-cadherin* and *MMP-9*, as determined by RT-qPCR and WB (**Fig. 6E**, **Supplementary Fig. 7D**). The coculture with, *M. bovis-infected* BoMac cells enhanced the migratory and invasive properties of EBL cells, as demonstrated by Transwell assay (**Figs. 6F and G**).

To confirm the impact of *RBMX2* knockout on the EMT process in the coculture model, we observed that *RBMX2* knockout cells exhibited significant upregulation of the epithelial cell marker protein *E-cadherin* and downregulation of the mesenchymal cell marker *N-cadherin* and *MMP-9* compared to WT EBL cells, as shown by RT-qPCR and WB (**Fig. 6H** and **Supplementary Fig. 7E**). Wound healing and Transwell assays demonstrated that the migration and invasion rates of *RBMX2* knockout cells were markedly lower than those of WT EBL cells (**Figs. 6I, J, and** K).

Finally, we silenced RBMX2 in the human lung cancer epithelial cell line H1299, which expresses high levels of RBMX2, to assess the effect on EMT-related proteins, as well as invasion and migration ability following *M. bovis* infection. The results indicated that RBMX2 significantly inhibited the EMT process in H1299 cells post-infection (**Supplementary Figs. 8A** and **B**).

In conclusion, we successfully established a coculture model involving *M. bovis*-infected BoMac cells that induce EMT in EBL cells, thereby demonstrating that the host factor *RBMX2* effectively promotes the EMT process in this context.

RBMX2 facilitates the EMT process via the *p65/MMP-9* pathway

EMT enhances the migration and invasion capabilities of tumor cells [35-37]. Both p65 and *MAPK/p38/JNK* pathways have been shown to regulate the EMT process through various mechanisms. [38-41]. To elucidate the precise regulatory role of *RBMX2* in the EMT process

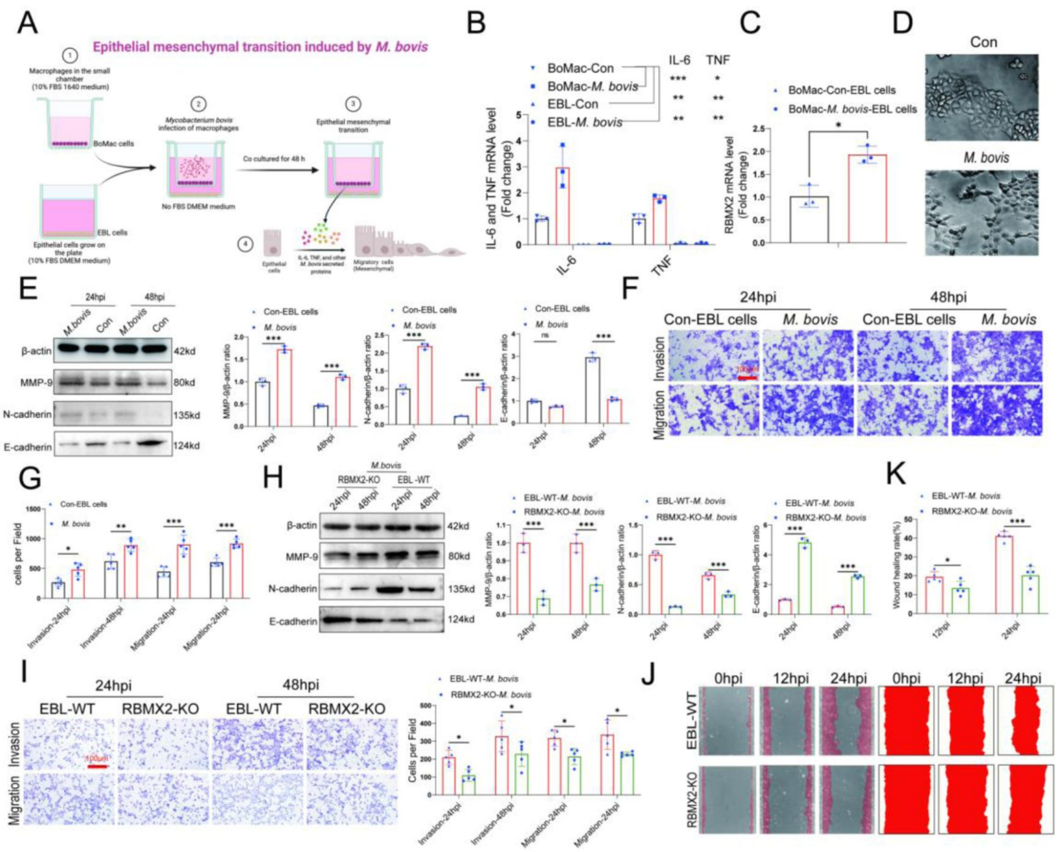

Figure 6

RBMX2 facilitates EMT process in EBL cells after *M. bovis*-infected BoMac cells.

(A) A pattern diagram illustrated a *M. bovis*-infected BoMac cells inducing EMT of EBL cells coculture model, drawing by BioRender. (B) Detection of IL-6 and TNF expression levels in EBL cells and BoMac cells infected with *M. bovis* using RT-qPCR. Data were relative to BoMac cells without infection of *M. bovis*. (C) Detection of RBMX2 expression levels in a coculture model EBL cells after *M. bovis* infection using RT-qPCR. Data were relative to BoMac cells without infection of *M. bovis*. (D) Observation of morphological changes in EBL cells infected with *M. bovis* under electron microscopy. (E) EMT-related proteins (*MMP-9*, *N-cadherin*, and *E-cadherin*) expression was verified in coculture model EBL cells after *M. bovis* infection through WB. Data were relative to coculture model EBL cells without *M. bovis* infection. (F, G) The impact of coculture model EBL cells after *M. bovis* infection on migration and invasion capacity was detected using Transwell assay. Data were relative to coculture model EBL cells without *M. bovis* infection. (H) The detection of EMT-related proteins (*MMP-9*, *N-cadherin*, and *E-cadherin*) of *RBMX2* knockout EBL cells after *M. bovis-infected* BoMac cells via WB. Data were relative to WT EBL cells after *M. bovis-infected* BoMac cells. (I) The change in the migratory and invasive capabilities of *RBMX2* knockout EBL cells after *M. bovis-infected* BoMac cells was assessed via Transwell assay. Data were relative to WT EBL cells after *M. bovis-infected* BoMac cells. (J, K) Validate the changes in migration abilities of *RBMX2* knockout EBL cells after *M. bovis-infected* BoMac cells through wound healing assay. Data were relative to WT EBL cells after *M. bovis-infected* BoMac cells. T-test and two-way ANOVA were used to determine the statistical significance of differences between different groups. Ns presents no significance, * presents $p < 0.05$, **presents $p < 0.01$, and *** presents $p < 0.001$ indicate statistically significant differences. Data were representative of at least three independent experiments.

within the coculture model of EBL cells, we assessed the *MAPK* pathway and p65 protein levels via WB. Our findings revealed a significant reduction in the phosphorylation of *p65* and *MAPK/p38/JNK* in *RBMX2* knockout cells infected with *M. bovis,* compared to WT EBL cells (**Supplementary Fig. 8C**).

To determine the specific pathways regulating the EMT phenotype of p65 and *MAPK/p38/JNK* in the coculture model, *RBMX2* knockout EBL cells were treated with *PMA*, *Anisomysin*, and *ML141*. We observed that p65 downregulates the expression level of *E-cadherin* while simultaneously upregulating *MMP-9* expression (**Fig. 7A**). The *MAPK/p38* pathway inhibits *E-cadherin* expression while promoting *N-cadherin* expression. Conversely, the *MAPK/JNK* pathway impedes *N-cadherin* expression while facilitate the expression of *E-cadherin and MMP-9*. Furthermore, we comprehensively investigated the correlation between pathway activation and the migration and invasion of phenotypes, demonstrating that the activation of the p65 pathway enhances the migratory and invasive capabilities of EBL cells, as evidenced by the Transwell assay (**Figs. 7B and C**) and wound-healing assay (**Figs. 7D and E**).

Invasion and migration are critical stages in tumor development, influenced by *p65*-dependent factors such as matrix metalloproteinases, urokinase fibrinogen activators, and interleukin-8 [42-46]. To further substantiate the correlation between the p65 protein and the regulation of the EMT process in EBL cells post-*M. bovis* infection, we employed siRNA to inhibit p65 expression in WT EBL cells. This suppression was found to inhibit *MMP-9* expression, as demonstrated by WB (**Figs. 7F and G**).

To verify the regulatory mechanism between *RBMX2* and *p65*, we first identified multiple amino acid residues in the *RBMX2* promoter that form strong interactions through docking (**Fig. 7H**). Additionally, we queried the *RBMX2* promoter region for binding sites of the transcription factor p65 using JASPAR data, subsequently validating this interaction using a dual luciferase reporter plasmid system (**Fig. 7I**) and Chip-PCR (**Fig. 7J**). Notably, *RBMX2* and p65 exhibited multiple amino acid residues forming strong bonds in protein docking, yielding a docking score of 1978.643 (**Fig. 7K**).

Moreover, MMP-9 is known to induce EMT in epithelial cells, enhancing their invasiveness. The regulatory mechanisms involving p65 and *MMP-9* have been documented in several studies [47, 48]. In our research, we identified multiple binding sites in the promoter sequences of p65 and MMP-9 through molecular docking (**Fig. 7L**) and confirmed the biding site between *MMP-9* promoter and *p65* protein via Chip-PCR (**Fig. 7M**). Using protein docking, we validated the relationship between bovine p65 protein and MMP-9, with a binding score of 1784.378 (**Fig. 7N**).

In summary, *RBMX2* facilitates the EMT process of EBL cells following *M. bovis* infection by activating the *p65/MMP-9* pathway.

Discussion

The resurgence of *M. bovis*-associated TB presents a substantial global challenge, affecting both livestock and human populations. Notably, *M. bovis* exhibits over 99% nucleotide similarity with *M. tb* [49]. The pathogenesis of TB is complex process influenced by a confluence of bacterial, host, and environmental factors. Both *M. tb* and *M. bovis* have evolved sophisticated strategies to evade host immune responses, enabling their long-term intracellular persistence. It is estimated that approximately one-third of the global population harbors latent TB infections [50, 51].

The successful establishment of infection by mycobacteria is contingent upon their ability to circumvent early innate immune defenses, employing both transcriptional and post-transcriptional regulatory strategies within host macrophages [52-56]. Despite notable

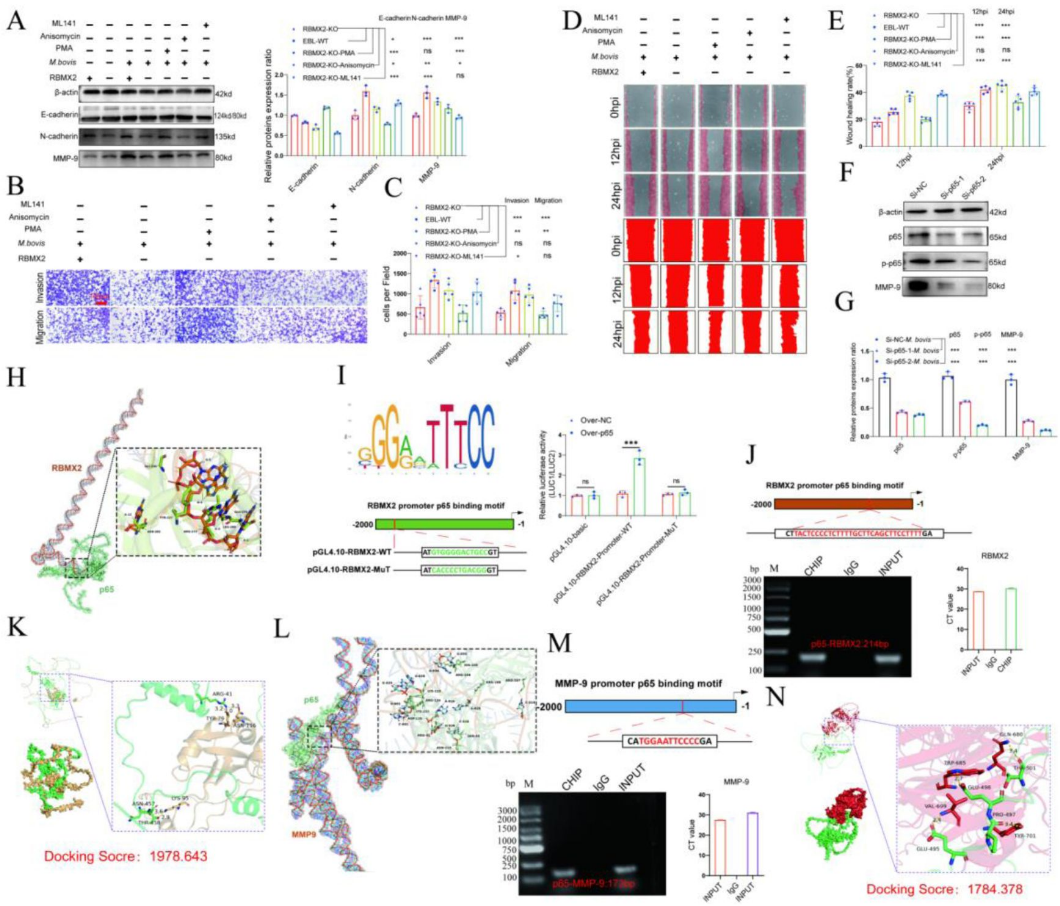

Figure 7

RBMX2 facilitates the EMT in EBL cells via *p65/MMP-9* pathway.

(A) Evaluate the impact of pathway activations on expression of EMT-associated proteins (*MMP-9*, *N-cadherin*, and *E-cadherin*) in *RBMX2* knockout EBL cells after *M. bovis-infected* BoMac cells. Data were relative to *RBMX2* knockout EBL cells untreated activators. (B, C) Evaluate the impact of pathway activations on the migratory and invasive capabilities of RBMX2 knockout EBL cells after *M. bovis-infected* BoMac cells via Transwell assay. Data were relative to *RBMX2* knockout EBL cells untreated activators. (D, E) Evaluate the impact of pathway activations on the migratory capabilities of *RBMX2* knockout EBL cells after *M. bovis-infected* BoMac cells via wound healing assay. Data were relative to *RBMX2* knockout EBL cells untreated activators. (F, G) The impact of p65 silencing on the expression of *MMP-9* protein in WT EBL cells after *M. bovis* infection was assessed using WB. Data were relative to SiRNA-NC in WT EBL cells with *M. bovis* infection. (H) Predicting the binding ability of RBMX2 promoter and p65 using molecular docking dynamics (I) Verification of *RBMX2* promoter region and p65 interaction using dual luciferase reporter system. (I) Using p65 antibody to precipitate p65 protein in EBL cells, and verification of *RBMX2* promoter region and p65 interaction using Chip-PCR assay. (K) Predicting potential binding sites for p65 and *RBMX2* via protein docking. (L) Verification of MMP-9 promoter region and p65 interaction using dual luciferase reporter system. (M) Verification of MMP-9 promoter region and p65 interaction using Chip-PCR. (N) Predicting potential binding sites for p65 and *MMP-9* via protein docking. Two-way ANOVA was used to determine the statistical significance of differences between different groups. *p < 0.05, **p < 0.01, and ***p < 0.001 indicate statistically significant differences. Data were representative of at least three independent experiments.

advancements in the field, unraveling the mechanisms of immune evasion and understanding the dynamics of latent infections caused by *M. tb* and *M. bovis* remains a substantial challenge. The cellular immune response to these pathogens is inherently complex, further compounded by the microdiversity of mycobacteria within individual hosts and the variability of immune responses among different individuals [54, 57].

Lung epithelial cells serve as the primary physical barrier against infection and play a pivotal role in the innate immune response. These cells not only function as a frontline defense but also recruit and activate antigen-presenting cells, such as macrophages, to initiate adaptive immune responses against *M. bovis* infection [58, 59]. Given that alveolar epithelial cells can act as reservoirs for *M. bovis*, their role in the infection process is particularly significant. Additionally, activated macrophages and neutrophils enhance the bactericidal effects of alveolar epithelial cells, further contributing to the host's defense mechanisms [60, 61].

In our study, we utilized a CRISPR-Cas9 mutant library developed in our laboratory to investigate potential host factors influencing M. bovis infection. Notably, we identified *RBMX2* as a protein with significant anti-*M. bovis* infection capabilities. The *RBMX2* protein, characterized by an RNA recognition motif within its 56-134 amino acid residue region, is implicated in mRNA splicing through spliceosomes and is emerging as a potential molecular marker for sperm activity.[62]. The downregulation of RBMX2 in the X chromosome of lung telocytes suggests its involvement in cellular immunity [63].

Further exploration of RBM genes in cattle revealed that EIF3G, RBM14, RBM42, RBMX44, RBM17, PUF60, SART3, and RBM25 belong to the same subfamily as RBMX2. Previous studies have demonstrated that genes within this subfamily can regulate the proliferation and lifecycle of cancer cells. For instance, EIF3G modulates the mTOR signaling pathway, inhibiting the proliferation and metastasis of bladder cancer cells [64]. Similarly, RBM14 has been linked to the reprogramming of glycolysis in lung cancer, acting as a novel epigenetically activated oncogene [60]. Despite these insights, the specific function of RBMX2 in the context of *M. bovis* infection and its potential role in cancer pathogenesis remain largely unexplored.

Our findings reveal that RBMX2 is upregulated in TB-infected cells and tissues, demonstrating the capacity to inhibit *M. bovis* invasion. Transcriptomic analyses indicate that RBMX2 may disrupt tight junctions within epithelial cells and promote epithelial-mesenchymal transition (EMT) following *M. bovis* infection.

Our findings reveal that *RBMX2* is upregulated in TB-infected cells and tissues, demonstrating its capacity to inhibit *M. bovis* invasion. Transcriptomic analyses suggest that *RBMX2* may disrupt tight junctions within epithelial cells and promote EMT following *M. bovi*s infection.

Epithelial cells serve as more than passive barriers; they actively participate in innate immunity by regulating cytokine secretion and maintaining barrier integrity [61]. Disruptions in epithelial tight junctions, often exacerbated by pro-inflammatory stimuli from pathogenic bacteria, can facilitate bacterial translocation and subsequent infection [61, 65, 66]

In our experiments, we observed that the disruption of the epithelial barrier facilitated *M. bovis* adhesion and invasion. Conversely, the knockout of RBMX2 stabilized the epithelial barrier, attenuating *M. bovis* invasion and intracellular survival. This stabilization also mitigated downstream innate immune responses, reducing cellular inflammation, ROS production, and apoptosis.

The loss of tight junction integrity is a precursor to EMT, a process increasingly recognized for its role in cancer progression [20, 65-67]. Recent studies have established a link between bacterial infections and EMT induction, particularly in the context of gastric adenocarcinomas [68, 69].

Epidemiological evidence suggests that TB may serve as a risk factor for lung cancer [70, 71]; however, the underlying cellular mechanisms remain elusive. Chronic TB infection has been implicated in lung carcinogenesis, with reports indicating that BCG vaccination can enhance the survival of tumor cells under inflammatory conditions [72, 73].

Moreover, *M. tb*-infected THP-1 cells have been shown to induce EMT in lung adenocarcinoma epithelial cells [74]. Chronic infection with *M. tb* is associated with oxidative stress and inflammatory cytokine production, fostering an environment conducive to tumor progression [75, 76]. Our analysis of RBMX2 across various cancers revealed increased expression levels in lung adenocarcinoma (LUAD) and lung squamous cell carcinoma (LUSC), suggesting a conserved role in tumor biology across species.

In light of these findings, we constructed a model of *M. bovis* infection in EBL cells to investigate EMT induction. Initial results indicated that *M. bovis* alone did not induce EMT; however, a co-culture model incorporating *M. bovis*-infected BoMac cells successfully induced EMT in EBL cells. Notably, the knockout of RBMX2 in this context inhibited EMT, suggesting that RBMX2 may elevate the risk of lung cancer through EMT induction following *M. bovis* infection.

In conclusion, our study identifies *RBMX2* as a novel host factor influencing susceptibility to *M. bovis* infection, playing a crucial role in both TB pathogenesis and the EMT process associated with lung cancer. Targeting RBMX2 may present a promising avenue for the prevention and treatment of TB in both humans and animals. Additionally, the effective modulation of *RBMX2* could potentially mitigate the incidence of TB-associated EMT and its implications for lung cancer development in the near future.

Conclusion

Our findings demonstrate that *RBMX2* significantly facilitates the invasion of *M. bovis* by promoting the activation of the p65 protein. This activation undermines the integrity of the epithelial cell barrier and promotes the EMT of epithelial cells through the *p65/MMP-9* signaling pathway. These insights elucidate the critical role of RBMX2 in *M. bovis* pathogenesis and highlight its potential as a therapeutic target for mitigating infection-related complications.

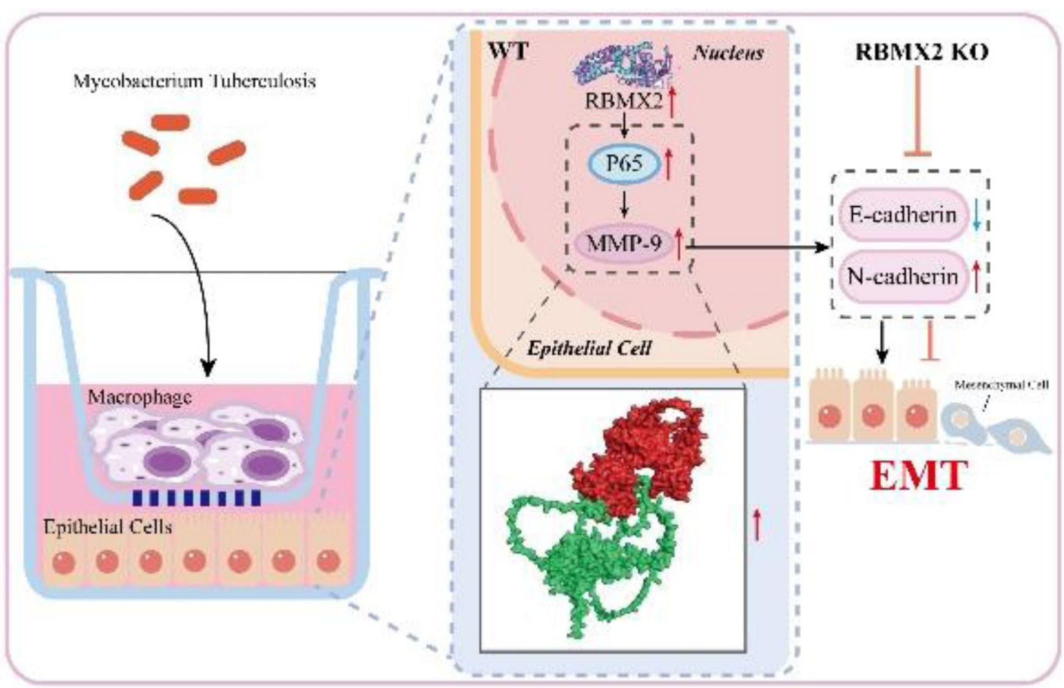

Methods

Patients and lung tissues

This study was approved by the Ethics Committee of Inner Mongolia Autonomous Region People's Hospital, and written informed consent was obtained from all participating patients (Approval Number: No. 2020021). A total of 35 specimens of lung cancer tissue, along with adjacent normal lung tissue, were collected. We randomly selected the above specimens, including age and gender. All patients involved in this study had not received any medication, chemotherapy, or radiation therapy prior to surgical resection. The samples were subsequently prepared for immunohistochemistry (IHC) and fluorescence in situ hybridization (FISH) assays.

Bovine clinical tissues

This project has received approval from the Experimental Animal Ethics Center of Huazhong Agricultural University (Approval Number: HZAUCA-2024-0014). Following examination by researchers at the National Animal Tuberculosis Professional Laboratory (Wuhan), bovine tuberculosis tissue samples were collected from the lungs and livers of slaughtered cattle, with each specimen measuring at least 5 cm × 5 cm × 5 cm and specifically including tissues exhibiting tuberculous lesions.

Cell lines

EBL and 293T RRID:CVCL_0063 cells were generously provided by M. Heller from Friedrich-Loeffler-Institute. These cells were cultured in heat-inactivated 10% fetal bovine serum supplemented with Dulbecco's modified Eagle medium (DMEM, Gibco, USA) at 37°C and 5% CO_2[77]. BoMac cells were kindly provided by Judith R. Stabel from the Johne's Disease Research Project at the United States Department of Agriculture in Ames, Iowa, and were maintained according to previously established protocols[78]. BoMac cells were grown in heat-inactivated 10% fetal bovine serum supplemented with Roswell Park Memorial Institute 1640 (RPMI 1640, Gibco, USA) at 37°C and 5% CO_2. Bovine lung alveolar primary cells were isolated in our laboratory and cultured in heat-inactivated 10% fetal bovine serum supplemented with DMEM (Gibco, USA) at 37°C and 5% CO_2. BEAS-2B RRID:CVCL_0168, NCIH1299, NCIH460 RRID:CVCL_0459, and CALU1 epithelial cells were all provided by Professor Shi Lei from Lanzhou University, and all culture procedures were conducted according to standardized protocols. We conduct regular testing on all cell lines to eliminate contamination from mycoplasma and black fungus.

Bacterium

M. bovis (ATCC:19210), originally isolated from a cow, is maintained in this laboratory. *M. smegmatis* mc[2]155 (NC_008596.1) and *M. bovis* BCG-Pasteur (ATCC:35734) were generously provided by Professor Luiz Bermudez from Oregon State University. All strains were cultured in a Middlebrook 7H9 broth (BD, MD, USA) supplemented with 0.5% glycerol (Sigma, MO, USA), 10% oleic acid–albumin–dextrose–catalase (OADC, BD, USA) and 0.05% Tween 80 (Sigma, MO, USA) or on Middlebrook 7H11 agar plates (BD, MD, USA) containing 0.5% glycerol (Sigma, MO, USA) and 10% OADC (BD).

Prior to infection, the optical densities of bacterial cultures at 600 nm (OD600) were adjusted to the required MOI using the standard turbidimetric card. The cultures were then centrifuged at 3,000 g for 10 min. The precipitated bacteria were resuspended in medium and dispersed using an insulin syringe. Subsequently, 50 μL of 10-fold serially diluted bacterial suspension was plated onto Middlebrook 7H11 agar to determine the number of viable bacteria (colony-forming units, CFUs).

All experiments involving *M. bovis* were conducted in strict accordance with the biosafety protocols established for the Animal Biosafety Level 3 Laboratory of the National Key Laboratory of Agricultural Microbiology at Huazhong Agricultural University.

E. coli (ATCC:25922) was donated by Professors Zhou Rui and Wang Xiangru of Huazhong Agricultural University, while *Salmonella* (ATCC:14028) has been preserved and passed down through generations in our laboratory. These strains were resuscitated, and single colonies were purified, cultured, and grown in Luria–Bertani broth.

Generation of the *RBMX2*-KO EBL cells

The small guide RNA (sgRNA) sequence targeting the bovine *RBMX2* gene (5'-GAATGAGCGTGAGGTCGAAC-3') was cloned into the pKLV2-U6gRNA5 (BbsI)-PGKpuro2ABFP (#67991), kindly provided by Professor Zhao Shuhong of Huazhong Agricultural University, to construct the recombined lentivirus. EBL cells were then infected with either the *RBMX2* pKLV2-U6gRNA5(BbsI)-PGKpuro2ABFP (#67991) lentivirus or the empty vector pKLV2-U6gRNA5(BbsI)-PGKpuro2ABFP (#67991) lentivirus as a negative control. After 48 to 60 hpi, puromycin (2.0 mg/mL) was added to select the positive clones. Finally, the monoclonal cells obtained through limiting dilution were expanded, and the knockout of RBMX2 was confirmed via PCR assay (**Table S1**).

Table S1

sgRNA	sequence
sgRNA-F	5'-CCTTGCCCAATTTTTCGGAGG-3'
sgRNA-R	5'-ACAGGAGGATGGTAGTAACGG-3'

Extraction of total RNA and RT-qPCR

Cold phosphate-buffered saline (PBS, HyClone, China) was used to wash the cells three times, after which 1 mL of Trizol (Invitrogen, USA) was added per well to lyse the cells. The lysate was collected in EP tubes, and 200 μL of chloroform was subsequently added. The mixture was vortexed for 30 seconds and then centrifuged at 12,000 rpm for 10 minutes at 4°C. Following centrifugation, 500 μL of the supernatant was transferred to a new EP tube. To this supernatant, 500 μL of isopropanol was added and mixed gently by inversion. The mixture was allowed to stand for 10 minutes at 4°C before being centrifuged again at 12,000 rpm for 15 minutes at 4°C. The supernatant was discarded, revealing the RNA pellet. Next, the RNA pellet was washed with 1 mL of 75% ethanol and centrifuged at 7,500 rpm for 5 minutes at 4°C. The supernatant was removed, and the RNA pellet was air-dried for 15 minutes. Subsequently, 20 μL of DEPC-treated water was added, and the mixture was incubated at 58°C in a water bath for 10 minutes to dissolve the RNA. Purified RNA was then obtained.

To assess RNA purity, the OD260/OD280 ratio was measured using a NanoDrop ND-1000 instrument (Agilent Inc., USA), with values between 1.8 and 2.0 indicating acceptable purity. RNA integrity and potential contamination with genomic DNA were evaluated using denaturing agarose gel electrophoresis. The samples were stored at -80°C for later analysis.

Reverse transcription of the RNA samples was performed using HiScript III RT SuperMix for qPCR (+gDNA wiper, Vazyme, China). Four microliters of 4× gDNA wiper mix were added to 1 μg of RNA, followed by the addition of 16 μL of RNase-free ddH2O. The mixture was incubated at 42°C for 2 minutes to eliminate genomic DNA. Reverse transcription was subsequently carried out by adding 4 µL of 5× HiScript III qRT SuperMix, with the mixture incubated at 37°C for 15 minutes and then at 85°C for 5 seconds to synthesize cDNA.

cDNA expression across different sample groups was quantified using AceQ qPCR SYBR Green Master Mix (Vazyme, China) in a ViiA7 real-time PCR machine (Applied Biosystems Inc., USA). The final volume of each real-time PCR reaction was 20 µL, comprising 10 µL of 2× AceQ qPCR SYBR Green Master Mix, 0.4 µL of upstream primer (10 µM), 0.4 µL of downstream primer (10 µM), 0.4 µL of 50× ROX reference dye 2, 3 µL of cDNA template, and 5.8 µL of ddH_2O. The PCR conditions were as follows: 95°C for 5 minutes (1 cycle), 95°C for 10 seconds (40 cycles), and 60°C for 30 seconds (40 cycles). The primer sequences for RT-qPCR are provided in **Table S2**.

Western blot

RIPA reagent (Sigma, USA), supplemented with protease inhibitors and phosphatase inhibitors (Roche, China), was added to the cell samples, and the cells were lysed on ice for 30 minutes. The supernatant was collected by centrifugation at 12,000 rpm and 4°C for 10 minutes. Protein concentrations of each sample were determined using a BCA kit (Beyotime, China), and the proteins were adjusted to equal concentrations.

The protein samples were mixed with 5× protein loading buffer and boiled for 10 minutes. Proteins were then separated using SDS-PAGE on 10% polyacrylamide gels at 100 V for 90 minutes, followed by transfer to polyvinylidene difluoride (PVDF) membranes (Millipore, Germany) at 100 V for 70 minutes. The PVDF membrane was incubated in 5% skimmed milk for 4 hours to block non-specific binding. The membrane was washed three times with Tris-buffered saline containing 0.15% Tween-20 (TBST) for 5 minutes each.

Subsequently, the membrane was incubated with a primary antibody at 4°C for 12 hours, followed by a secondary antibody at room temperature for 1 hour. The following primary antibodies were utilized: ZO-1 (Bioss, China), OCLN (Proteintech, China), CLADN-5 (Proteintech, China), MMP-9 (Proteintech, China), E-cadherin (Proteintech, China), N-cadherin (Bioss, China), LaminA/C (Proteintech, China), β-actin (Bioss, China), p65 (CST, USA), p-p65 (CST, USA), and a MAPK-related antibody (CST, USA). The following secondary antibodies were used: anti-mouse HRP secondary antibody and anti-rabbit HRP (Invitrogen, USA).

Phylogenetic tree construction and gene structure and function predictive analysis of the bovine RBM family

The bovine RBM protein sequences were converted into FASTA format files and imported into MEGA-X for comparative analysis. The neighbor-joining method was employed to construct the phylogenetic tree of the CsGRF protein. The iTOL website (*https://itol.embl.de/*) was utilized to enhance the visualization of the CsGRF phylogenetic tree. Additionally, the MEME Suite database (*http://meme-suite.org/*) was used for the online analysis of conserved motifs within the RBM gene family.

Adhesion assay

EBL cells were infected with different live bacteria at an MOI of 20 for durations of 15 minutes, 30 minutes, 1 hour, and 2 hours at 4°C. Following infection, the cells were washed three times with phosphate-buffered saline (PBS; Gibco, USA) to remove any extracellular bacteria. After thorough washing, cell lysis was achieved using 0.1% Triton X-100 (Beyotime, China). The resulting cell lysates were plated onto 7H11 or LB agar plates and incubated for several days to facilitate colony-forming unit (CFU) enumeration.

Number	Primer	Sequence
1	Bovine-β-actin-F	5′-AGCAAGCAGGAGTACGATGAG-3′
2	Bovine-β-actin-R	5′-ATCCAACCGACTGCTGTCA-3′
3	Human-β-actin -F	5′- CACCATTGGCAATGAGCGGTTC-3′
4	Human-β-actin -R	5′- AGGTCTTTGCGGATGTCCACGT-3′
5	Bovine-RBMX2-F	5′-TCCCACCGGCACAAAAAGTC-3′
6	Bovine-RBMX2-R	5′-TCAGTGATACCTGAGCTCCC-3′
7	Human-RBMX2-F	5′-ACCCCCTCACCAAGTTTGTC-3′
8	Human-RBMX2-R	5′-GTGCTTCTTAGGGCCAGTGT-3′
9	Bovine-HSPB8-F-1	5′-GACCAAGGACGGATACGTGG-3′
10	Bovine-HSPB8-R-1	5′-AGTTCTTGGAGACGATGCCC-3′
11	Bovine-ST14-F-1	5′-CTCGGCGCTGGATTCAAGTA-3′
12	Bovine-ST14-R-1	5′-CAAGAACTCCACGCCTTCCT-3′
13	Bovine-MUC16-F-1	5′-TGTGCATGTGACAGCAGAGC-3′
14	Bovine-MUC16-R-1	5′-CTGGAAACTGGGAGTGGTCG-3′
15	Bovine-TNC-F-1	5′-TGGCATCGGAGAATGCCTTT-3′
16	Bovine-TNC-R-1	5′-CAGCTTCCTCTGGGTTCCTG-3′
17	Bovine-GPX2-F-1	5′-ACCCGTTTTCCCTCATGACC-3′
18	Bovine-GPX2-R-1	5′-CGGCCCAATGAGGAACTTCT-3′
19	Bovine-THBS2-F-1	5′-GGGGACGCTTGTAAAGACGA-3′
20	Bovine-THBS2-R-1	5′-AATCTGAGTGGTGCCCTTGG-3′
21	Bovine-IL-7-F-1	5′-GCAATTGCCTGAATAACGAACCT-3′
22	Bovine-IL-7-R-1	5′-TTACCCTTGCTGGTGCAGTT-3′
23	Bovine-IL-24-F-1	5′-GACGCCTGCCCAACTTTCTT-3′
24	Bovine-IL-24-R-1	5′-AAGGGATGCTTGAGGGCTTG-3′
25	Bovine-FRMD4B-F-1	5′-CAGAGACAGGAGCACCAAGG-3′
26	Bovine-FRMD4B-R-1	5′-TTAAACTGCCGTTGCTTGCC-3′

Table S2

27	Bovine-OMD-F-1	5′-GCTCAACGTTGGACACAACA-3′
28	Bovine-OMD-R-1	5′-AGCTTATTGGCGCTTTCAGC-3′
29	Bovine-NOS3-F-1	5′-GTTCCCTCGCGTGAAGAACT-3′
30	Bovine-NOS3-R-1	5′-CTGGTTGATGAAGTCCCTGGC-3′
31	Bovine-MCTP1-F-1	5′-AGTTCCGACTTGGGCATCAG-3′
32	Bovine-MCTP1-R-1	5′-TACTGAGAGCCGACAGGTCA-3′
33	Bovine-MFAP5-F-1	5′-TGATATCCAGCCTTCCACCG-3′
34	Bovine-MFAP5-R-1	5′-CCGATGCACGGAGTAGAGTC-3′
35	Bovine-MMP-9-1-F	5′-CGCTATGGCTACACTCCTGG-3′
36	Bovine-MMP-9-1-R	5′-TGAGTTCGCCCTCAAAGGTC-3′
37	Bovine-N-cadherin-1-F	5′-CACTGCGATTGATGCTGACG-3′
38	Bovine-N-cadherin-1-R	5′-TGCCACCGTGATAATGTCCC-3′
39	Bovine-E-cadherin 1-F	5′-CAGAAGATGACACCCGGGAC-3′
40	Bovine-E-cadherin 1-R	5′-AGCATCCAGGCCCCTATGTA-3′
41	Bovine-CLDN-5-F-1	5′-CCTGGACCACAACATCGTGA-3′
42	Bovine-CLDN-5-R-1	5′-GGAGTCGTACACCTTGCACT-3′
43	Bovine-OCLN-F-1	5′-CTTTCAAAAAGGGCTCCCGC-3′
44	Bovine-OCLN-R-1	5′-TGGATATTCCCTGATCCAGTCG-3′
45	Bovine-TJP1-F-1	5′-CTCAAGTTCCTGAAGCCCGT-3′
46	Bovine-TJP1-R-1	5′-TAGGATCACCCGACGAGGAG-3′
47	Bovine-TNF-F-1	5′-GAAGTTGCTTGTGCCTCAGC-3′
48	Bovine-TNF-R-1	5′-AACCAGAGGGCTGTTGATGG-3′
49	Bovine-IL-6-F-1	5′-CTTCTGCTTTCCCTACCCCG-3′
50	Bovine-IL-6-R-1	5′-TTCTGCCAGTGTCTCCTTGC-3′
51	Bovine-IL-1β-F-1	5′-AAAAGCTTCAGGCAGGTGGT-3′
52	Bovine-IL-1β-R-1	5′-AACTCGTCGGAGGACGTTTC-3′

Table S2 (continued)

Invasion assay

EBL cells were infected with various live bacteria at an MOI of 20 for durations of 2, 4, and 6 hours at 37°C. Following infection, gentamycin (Procell, China) was added at a concentration of 100 μg/mL for 2 hours to eliminate any extracellular bacteria. The infected cells were then washed three times with phosphate-buffered saline (PBS) (Gibco, USA) to remove remaining extracellular bacteria. After sufficient washing, the cells were lysed using 0.1% Triton X-100 (Beyotime, China). The resulting cell lysates were subsequently plated onto 7H11 or LB agar plates and incubated for several days to allow for colony-forming unit (CFU) enumeration.

Intracellular survival assay

EBL cells were infected with various live bacteria at an MOI of 20 for 6 hours at 37°C. Following infection, gentamycin (Procell, China) was added at a concentration of 100 μg/mL to eliminate extracellular bacteria for 2 hours. The infected cells were then washed three times with phosphate-buffered saline (PBS) (Gibco, USA) to remove any remaining extracellular bacteria, which is referred to as the 0-hour time point.

Subsequently, the infected cells were cultured in complete medium supplemented with Triton X-100 (0.1%) (Beyotime, China) at various time points: 0, 24, 48, and 72 hours hpi. Cell lysates were plated onto 7H11 or LB agar plates and allowed to incubate for several days to facilitate colony-forming unit (CFU) counting.

RNA-Seq, proteomics and metabolomics

Total RNA was isolated using Trizol Reagent (Invitrogen Life Technologies), and the concentration, quality, and integrity were determined using a NanoDrop spectrophotometer (Thermo Scientific). Three micrograms of RNA were used as input material for RNA sample preparation. Sequencing libraries were generated according to the following steps: mRNA was purified from total RNA using poly-T oligo-attached magnetic beads. Fragmentation was performed using divalent cations under elevated temperature in an Illumina proprietary fragmentation buffer. First-strand cDNA was synthesized using random oligonucleotides and Super Script II. Second-strand cDNA synthesis was subsequently performed using DNA Polymerase I and RNase H. The remaining overhangs were converted into blunt ends via exonuclease/polymerase activities, and the enzymes were removed. After adenylation of the 3' ends of the DNA fragments, Illumina PE adapter oligonucleotides were ligated for hybridization. To select cDNA fragments of the preferred length of 400–500 bp, the library fragments were purified using the AMPure XP system (Beckman Coulter, Beverly, CA, USA). DNA fragments with ligated adaptor molecules at both ends were selectively enriched using the Illumina PCR Primer Cocktail in a 15-cycle PCR reaction. The products were purified (AMPure XP system) and quantified using the Agilent high-sensitivity DNA assay on a Bioanalyzer 2100 system (Agilent). The sequencing library was then sequenced on the NovaSeq 6000 platform (Illumina) by Shanghai Personal Biotechnology Co., Ltd.

RNA sequencing services were provided by Personal Biotechnology Co., Ltd. Shanghai, China. The data were analyzed using the free online platform Personalbio GenesCloud (*https://www.genescloud.cn*). Proteomics and metabolomics were performed by METWARE.

Differential expression analysis of the transcriptome

HTSeq (0.9.1) RRID:SCR_005514 statistical methods were employed to compare the read count values for each gene, which served as the original expression measurements, while FPKM was utilized for normalization. Subsequently, differential gene expression was analyzed using DESeq (1.30.0) RRID:SCR_000154 under the following screening criteria: a fold change of |log2FoldChange| > 2 and a significant P-value < 0.05. We employed the R language Pheatmap (1.0.8) software package to conduct bidirectional clustering analysis of all differentially expressed genes across samples. A heatmap was generated based on the expression levels of the same gene in various samples and the expression patterns of different genes within the same sample, utilizing the Euclidean method for distance calculation and the complete linkage method for clustering. Data analysis was performed using the free online platform Personalbio GenesCloud (*https://www.genescloud.cn*).

GO and KEGG enrichment analysis

We mapped all genes to terms in the Gene Ontology (GO) database and calculated the number of differentially enriched genes for each term. GO enrichment analysis was conducted on the differentially expressed genes using the topGO package, where P-values were determined using the hypergeometric distribution method. A threshold of P-value < 0.05 was set to identify significant enrichment, allowing us to pinpoint GO terms associated with significantly enriched differential genes and to elucidate the primary biological functions they perform. Additionally, we employed ClusterProfiler (3.4.4) software to conduct KEGG pathway enrichment analysis for the differential genes, concentrating on pathways with a P-value < 0.05. The data analysis was carried out using the free online platform Personalbio GenesCloud (*https://www.genescloud.cn*).

Flow cytometry assay

Cells were washed with cold PBS and then centrifuged at 1,500 rpm for 5 minutes; the supernatant was discarded. The cells were fixed in 70% ethanol for 12 hours. Following fixation, the cells were centrifuged again at 1,500 rpm for 5 minutes, and the supernatant was removed. The cells were washed once with cold PBS.

For staining, a Cell Cycle and Apoptosis Analysis Kit (Beyotime, China) was utilized. The staining mixture was prepared with a total volume of 535 μL, comprising 500 μL of staining buffer, 25 μL of PI dye, and 10 μL of RNase A. The samples were incubated with the staining mixture at 37°C for 30 minutes prior to detection.

Cell viability assay

EBL cells were infected with *M. bovis* at an MOI of 100. Cell viability was assessed at 48, 72, 96, 120, and 144 hpi using the CCK-8 assay (Dojindo, Kumamoto, Japan).

At each time point, fresh medium containing 10% CCK-8 was added to a 96-well cell plate and incubated for 60 minutes at 37°C. The cell viability was then determined by measuring the absorbance at 450 nm. The percentage of cell viability was calculated using the following formula:

cell viability (%) = [A (infection group) − A (blank group)] / [A (infection group) A (blank group)] × 100

Wound-healing assay

Approximately 2×10^5 treated cells were added to a 6-well plate after EBL cells were cocultured with BoMac cells for 48 hours following *M. bovis* infection and subsequently digested with 1× trypsin. Once the cells were evenly spread, a cross was drawn along a ruler using a 200 μL pipette tip to create a wound.

The cells were washed three times with PBS (Gibco, USA) to remove any detached cells, and serum-free medium was added to each well. Images were taken at 0, 12, and 24 hours of culture, and the healing rate was calculated using ImageJ software.

Cell adhesion assay

To assess the level of cell adhesion between RBMX2 knockout and wild-type (WT) EBL cells after *M. bovis* infection, a cell adhesion assay was performed using a cell adhesion detection kit (Bestbio, China) according to the manufacturer's protocol. Matrigel (20 mg/L) was added to a 96-well plate at 100 μL per well. Subsequently, 3×10^4 cells were added to the adhesion plate and incubated in a CO2 incubator for 6 hours. After incubation, the wells were washed twice with PBS, and the adhered cells were stained with 10 μL of cell stain solution A for 2 hours at 37°C. The level of cell adhesion was quantified by measuring the absorbance at 560 nm.

Transwell assay

5×10^4 treated cells and 200 μL of serum-free medium were added to each upper chamber of a Transwell (Corning, USA), while 550 μL of complete medium was added to the lower chamber. The cells were incubated for 24 hours.

The following day, the upper chamber was removed, and 550 μL of 4% paraformaldehyde (Beyotime, China) was added for 30 minutes. After fixation, 550 μL of crystal violet dye (Beyotime, China) was added to each well for another 30 minutes. The upper chamber was then washed with PBS for 30 seconds and dried upside down with a cotton swab.

After drying, the membrane of the chamber was removed and placed on a glass slide, followed by the addition of a neutral gum seal. Three random fields of view were selected under the microscope for imaging, and the cell count was performed using ImageJ RRID:SCR_003070 software.

Crystal violet staining assay

EBL cells were infected with *M. bovis* at an MOI of 100. The surviving cells on six-well plates were then fixed with 4% paraformaldehyde (Beyotime, China). After fixation, the cells were stained with 0.1% crystal violet staining solution (Beyotime, China) and rinsed five times with PBS (Gibco, USA). The plates were placed in a 37°C oven for 6 hours before being photographed.

M. bovis infection of BoMac and coculture with EBL cells

BoMac cells were seeded into the upper chamber of a 0.4 μm pore size Transwell (Corning, USA) at a density of 3×10^4 cells per insert in RPMI 1640 medium supplemented with 10% FBS. The following day, the cells were infected with *M. bovis* at an MOI of 5 for 4 hours. After infection, the cells were washed three times with 1× warm PBS and treated with Gentamycin (100 μg/mL) for 2 hours to eliminate any extracellular bacilli.

The infected and uninfected BoMac cells were then incubated for 24 hours to mitigate the effects of *M. bovis* infection. Afterward, the cells underwent an additional 24-hour incubation period in fresh RPMI 1640 medium before coculturing with EBL cells.

In parallel, EBL cells were seeded at a density of 2×10^5 cells per well onto 12-well plates containing DMEM supplemented with 10% FBS. The following day, culture inserts containing either *M. bovis*-infected or uninfected BoMac cells were introduced into the wells of the 12-well plates containing EBL cells, and the coculture was incubated for up to 24 and 48 hours in serum-free DMEM.

Small interfering RNA (siRNA) transfection

EBL cells were transfected with p65 siRNA (Tsingke, China) using jetPRIME (Polyplus, France) following the manufacturer's instructions. Scrambled siRNA (Tsingke, China) served as a negative control.

Cells were seeded in 12-well plates and cultured at 37°C in a 5% CO_2 atmosphere. To prepare the transfection mixture, 0.8 μg of jetPRIME was incubated with 1 μL of siRNA for 10 minutes. This mixture was then added to the cells and incubated for 12 hours.

Following the incubation, RNA extraction was performed, and the efficiency of transfection was calculated.

The siRNA sequences used were as follows:

Cattle p65-1 siRNA, sense 5'-GCAGUUUGAUACCGAUGAA (dT)(dT)-3';

Cattle p65-1 siRNA, antisense 5'-UUCAUCGGUAUCAAACUGC (dT)(dT)-3';

Cattle p65-2 siRNA, sense 5'-GGACGUACGAGACCUUCAA (dT)(dT)-3';

Cattle p65-2 siRNA, antisense 5'-UUGAAGGUCUCGUACGUCC (dT)(dT)-3'.

P65 nuclear translocation assay

For the p65 nuclear translocation assay, RBMX2 knockout and wild-type cell lines were transfected with the pCMV-EGFP-p65 plasmid. Following transfection, bovine lung epithelial cells were infected with *M. bovis*.

After infection, the cell nuclei were stained with Hoechst dye. The entry of p65 into the nucleus was analyzed at different time points using a confocal high-resolution cell imaging analysis system from PerkinElmer Life and Analytical Sciences Ltd. (Britain). This imaging technique allowed for the assessment of p65 translocation into the nucleus in response to infection.

CHIP-PCR

Formaldehyde cross-linking and ultrasonic fragmentation of cells were performed. One plate of cells was removed, and the volume of the culture medium was measured. 37% formaldehyde was added to achieve a final concentration of 1%, and the plates were incubated at 37°C for 10 minutes. Glycine (2.5 M) was then added to the plates at a final concentration of 125 mM to terminate cross-linking. After mixing, the culture medium was left at room temperature for 5 minutes, and the cells were cleaned three times with cold PBS. The cells were scraped off with PBS, centrifuged at 2,000g for 5 minutes, and the supernatant was removed. IP lysis solution containing a protease inhibitor was added to lyse the cells (the amount of lysis solution depending on the amount of cell precipitation), and the mixture was fully lysed on ice for 30 minutes, with the cells being repeatedly blown with a gun or shaken on a vortex mixer to ensure complete lysis.

After sonication, the mixture was centrifuged at 12,000 rpm at 4°C for 10 minutes to remove insoluble substances and collect the supernatant. 90 μL of the input was retained, and the rest was stored at −80°C. To confirm the presence of the target protein in the sample, 40 μL of the ultrasonic crushing product was taken, mixed with 10 μL of L5 reduced protein loading buffer, and heated for denaturation before performing Western blot detection.

For the remaining 50 μL of the product, 5 μL of Protease K and 2 μL of 5M NaCl (final NaCl concentration of 0.2M) were added and incubated at 55°C overnight for cross-linking. After cross-linking, the nucleic acid concentration was measured, and a portion of the sample was taken for PCR amplification, followed by agarose gel electrophoresis to detect the effectiveness of ultrasonic fragmentation and confirm the presence of the target DNA. After verifying the Input result, 100 μL of the ultrasonic crushing products was frozen at −80°C.

Next, 900 μL of ChIP Diffusion Buffer containing 1 mM PMSF and 20 μL of 50% of 1× PIC was added, along with an additional 60 μL of Protein A+G Agarose/Salmon Sperm DNA. The mixture was stirred at 4°C for 1 hour, allowed to stand at 4°C for 10 minutes to precipitate, and then centrifuged at 4000 rpm for 5 minutes. The sample was divided into two 1.5 mL EP tubes; the target protein IP antibody was added to one tube, while IgG (1 μg of the corresponding species) was added to the other. The samples were shaken overnight at 4°C for precipitation and cleaning of immune complexes.

After the overnight incubation, 200 μL of Protein A+G Agarose/Salmon Sperm DNA was added to each tube, shaken at 4°C for 2 hours, allowed to stand at 4°C for 10 minutes, and then centrifuged at 4,000 rpm for 1 minute. The supernatant was removed, and 8 μL of 5M NaCl and 20 μL of Protein K were added for overnight cross-linking at 55°C. Using databases like JASPAR to predict transcription factor binding sites, primers were designed and synthesized based on these binding sites. RT-PCR was employed to verify the binding, and after amplification, the products were taken for gel electrophoresis to confirm the correct fragment size (**Table S3**).

Table S3

Gene name	Sequence
MMP9	5′-AGGCACTGAAGGAATGAGGC-3′
	5′-CCCCGCTTGGTGGAAAT-3′
RBMX2	5′-CTGACAGGAGGACCAGAGTTT-3′
	5′-TGCCTAGTTGTAGGGTTGAAGT-3′

Dual-luciferase reporter assay

293T cells in the logarithmic growth phase were adjusted to a density of 5 × 10^4 cells/mL and inoculated into 48-well cell culture plates, with 300 cells per well. Each concentration gradient was represented by three replicate wells. On the second day after plating, when the cells reached a density of approximately 60-70%, transfection was performed with the following experimental groups: pGL4.10 RRID:Addgene_72684 basic+pRL TK+Over NC, pGL4.10 basic+pRL TK+Over p65, pGL4.10-*RBMX2*-WT+pRL TK+Over NC, pGL4.10-*RBMX2*-WT+pRL TK+Over p65, pGL4.10-*RBMX2*-MUT+pRL TK+Over NC, pGL4.10-*RBMX2*-MUT+pRL TK+Over p65. Transfection complexes were prepared, and dual-luciferase detection was carried out 48 hours post-transfection.

For cell lysis, the cell culture medium was removed, and the cells were gently rinsed twice with PBS. Then, 50 μL of 1× PLB lysis solution was added to each well, and the plates were placed on a shaking table at room temperature for 15 minutes to ensure complete lysis.

From each sample, 20 μL was taken for measurement. To assess Firefly luciferase activity, 100 μL of Firefly luciferase detection reagent (LAR II reagent, Promega, USA) was added, mixed well, and the relative light unit (RLU1) was measured. After this, 100 μL of Sea Kidney luciferase detection reagent (1× Stop&Glo® Reagent, Promega, USA) was added, mixed thoroughly, and the relative light unit (RLU2) was measured.

The activation level of the target reporter genes was compared between different samples by calculating the ratio of RLU1 from the Firefly luciferase assay to RLU2 from the Sea Kidney luciferase assay.

Protein docking

Molecular docking simulations were conducted to predict the formation of stable complexes between proteins RBMX2 or MMP9 with p65. The aligned sequences of RBMX2, MMP9, and p65 proteins were sourced from the UniProt RRID:SCR_002380 database. Their three-dimensional structures were predicted using AlphaFold and refined by constructing the structures in Avogadro. The structures were then optimized using the MMFF94 force field and exported in PDB format for further optimization in Gauss09.

The docking of the proteins was performed using Hdock, where each protein was treated separately as the receptor and ligand to assess their interactions [79]. The resulting docking affinities were annotated to provide insight into the binding interactions. Finally, PyMOL RRID:SCR_000305 was utilized to visualize the binding interaction geometries, allowing for a detailed examination of the molecular interactions between the proteins.

Statistical analysis

Statistical analysis was performed on all assays conducted in triplicate, with data expressed as the mean ± standard error of the mean. Each experiment was independently repeated three times. GraphPad Prism 7.0 RRID:SCR_002798 (La Jolla) was utilized for statistical analysis, employing a two-tailed unpaired t-test with Welch's correction for comparisons between two groups. For comparisons among multiple groups, one-way or two-way ANOVA was applied, followed by the LSD test. Statistical significance was indicated at four levels: not significant (ns presents $p > 0.05$), * presents $p < 0.05$, ** presents $p < 0.01$, and *** presents $p < 0.001$.

Supplementary figures and tables

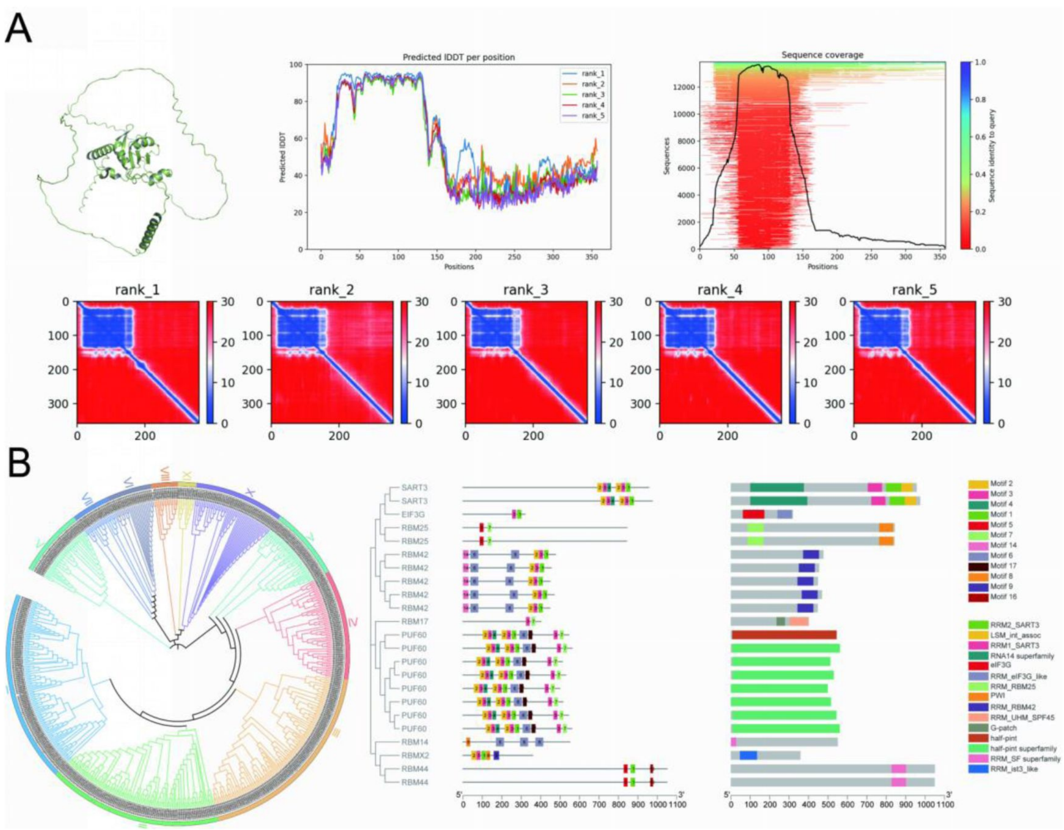

Supplementary Fig 1

Protein structure analysis, subfamily localization.

(A) AlphaFold Multimer predicted the sequence and structure of *RBMX2* protein. (B) Construction of RBM Gene Family Tree and structural Analysis of genes in *RBMX2* subfamily.

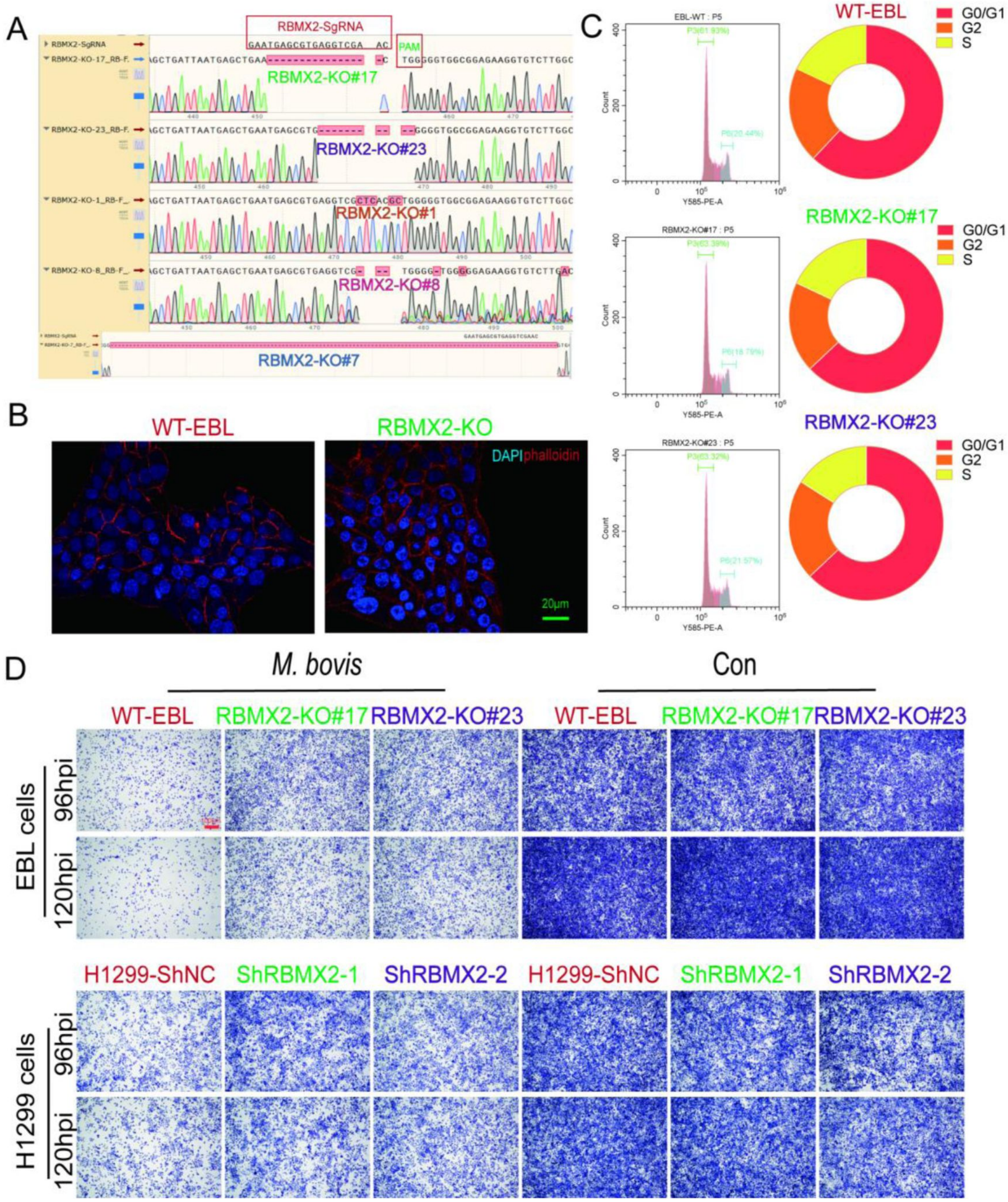

Supplementary Fig 2

The influence of *RBMX2* in cell cycle, cell morphology, cell proliferation, and resistance to *M. bovis* infection.

(A) The different knockout sites of *RBMX2* EBL cells were observed by sequencing compared to the bovine *RBMX2* sequence or WT EBL cells. (B) Using phalloidine to stain the EBL cell skeleton, observing cell morphology under a high-intensity microscope. The cytoskeleton is labeled with red fluorescence, and the nucleus is stained with blue fluorescence. Scale Bar: 20 μm. (C) Observation of the effect of *RBMX2* knockout on cell cycle of EBL cells by flow cytometry assay. Data are represented as the G0/G1 and S phase relative to WT EBL cells. (D) The change in cell number of *RBMX2* knockout and silence following 96 and 120 hours of *M. bovis* infection was observed via crystal violet assay in EBL cells and H1299 cells, respectively. Data were represented as the cell number relative to WT EBL cells and H1299-ShNC cells after *M. bovis*-infection. Data were representative of at least three independent experiments.

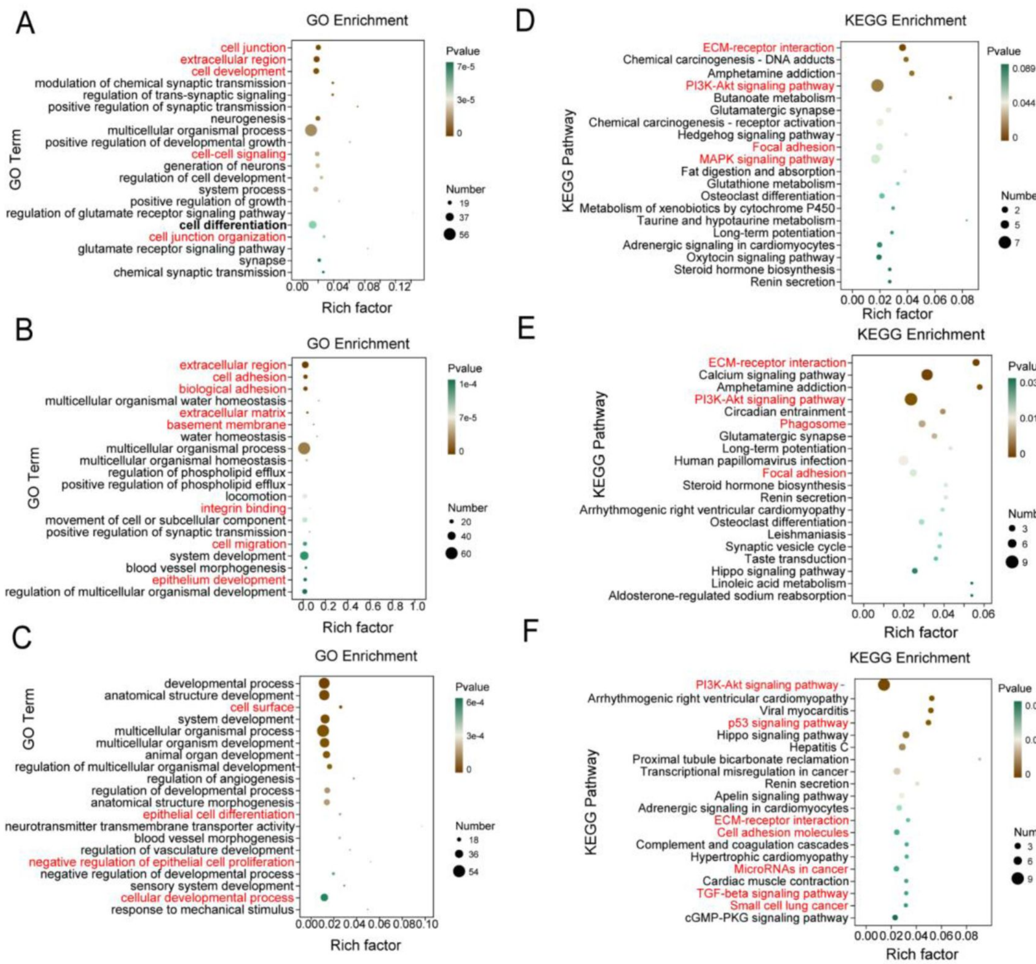

Supplementary Fig 3

Transcriptome analysis in *RBMX2* knockout and WT EBL cells after *M. bovis* infection in different time points.

(A-C) GO analysis of enriched genes of (A) 0, (B) 24 and (C) 48h after *M. bovis* infection, respectively. Data were in RBMX2 knockout EBL cells relative to WT EBL cells with *M. bovis* infection. The changes of these pathways from cell junction-related pathways in 0 hpi to cell proliferation and differentiation-related pathways in 48 hpi. (D-F) KEGG analysis of enriched genes of (D) 0, (E) 24 and (F) 48hpi after *M. bovis* infection, respectively. Data were in RBMX2 knockout EBL cells relative to WT EBL cells with *M. bovis* infection. The changes of these pathways from inflammation-related pathways in 0 hpi to cancer-related pathways in 48 hpi.

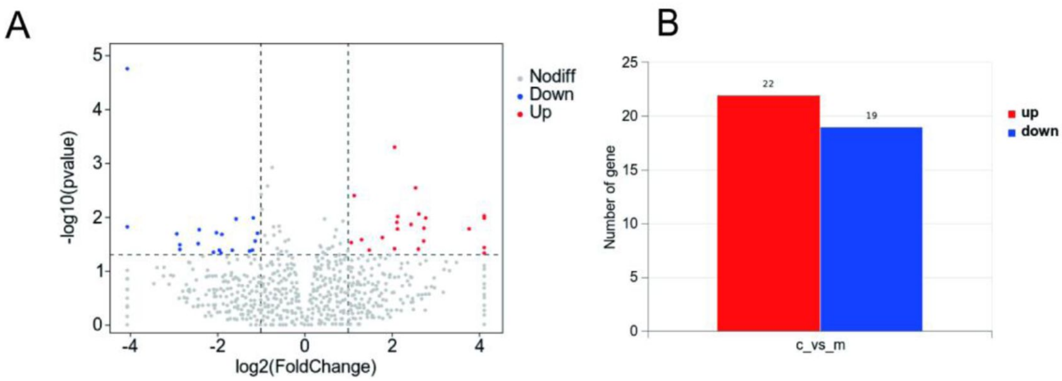

Supplementary Fig 4

Transcriptomic analysis of *M. bovis* infected EBL cells.

(A, B) A volcano map illustrating the transcriptional enrichment genes after WT EBL cells with *M. bovis*-infection. Data were relative to WT EBL cells without *M. bovis* infection.

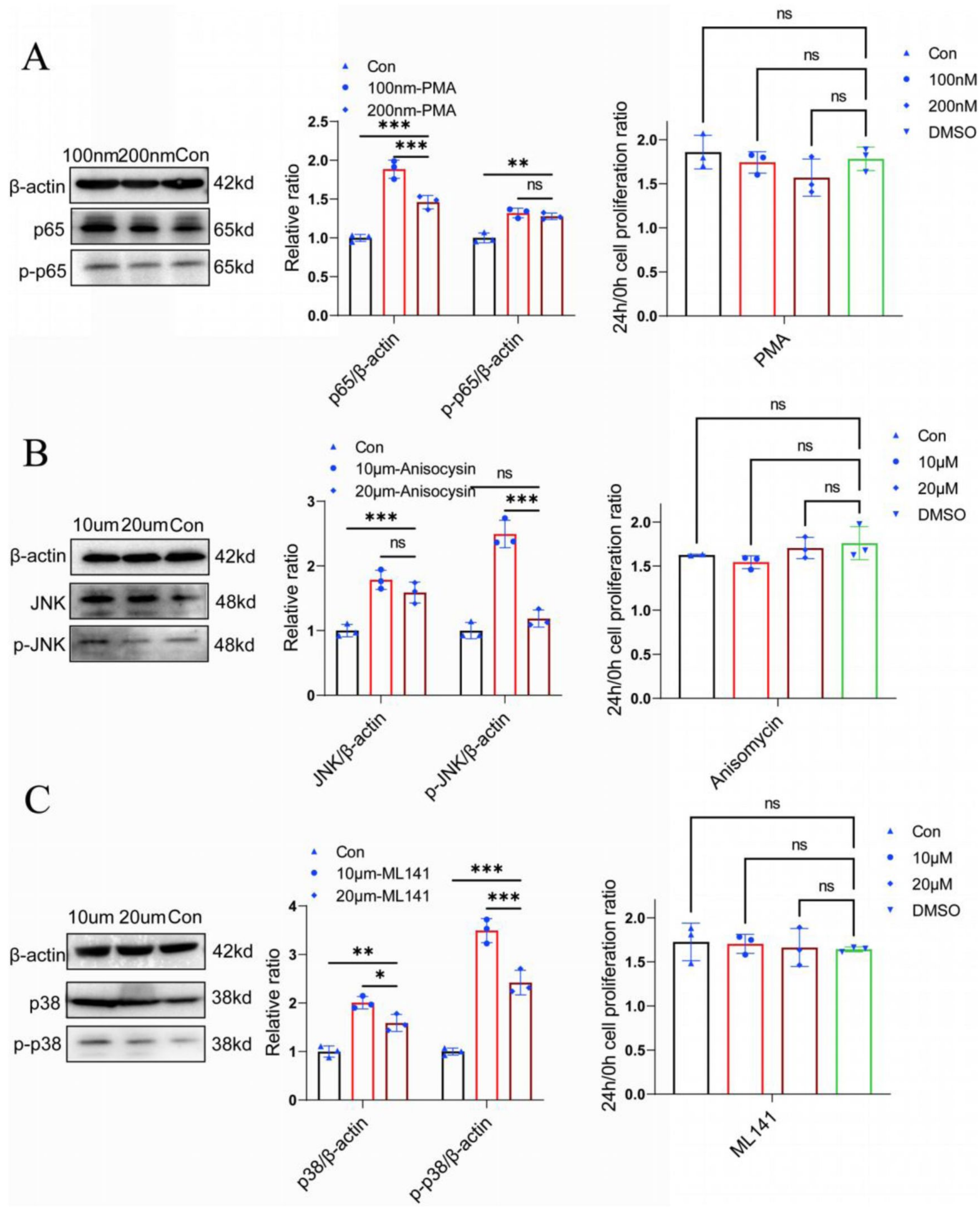

Supplementary Fig 5

The optimal concentration of activators and their impact on cell viability.

(A-C) Ascertain the optimal concentration of the three pathway activators and their impact on cellular viability via WB and CCK-8 assays. Data were relative to WT EBL cells untreated activators. One-way ANOVA was used to determine the statistical significance of differences between different groups. Ns presents no significance, **presents $p < 0.01$, and *** presents $p < 0.001$ indicate statistically significant differences.

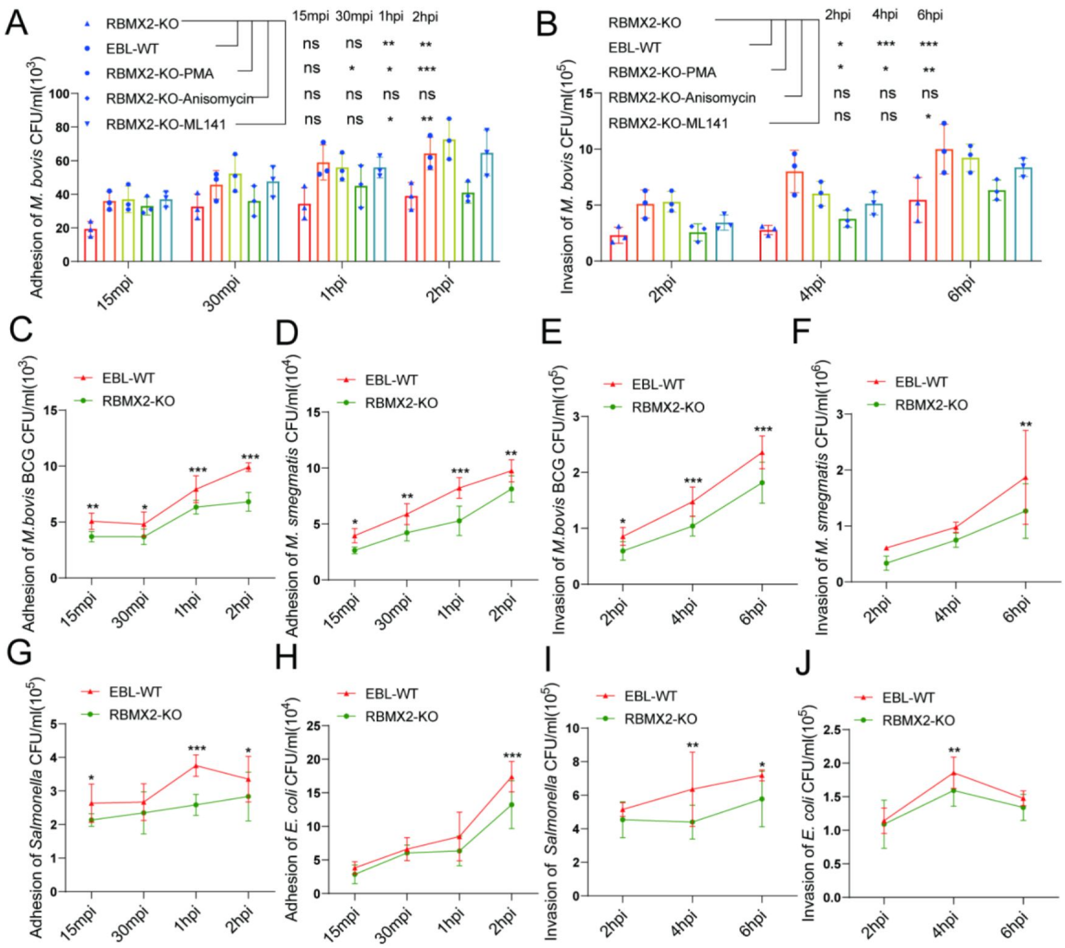

Supplementary Fig 6

RBMX2 enhanced the processes of pathogen adhesion, invasion, and intracellular survival.

(A, B) The impact of *M. bovis* on the adhesion and invasion of *RBMX2* knockout EBL cells following treatment with related-pathway activators, verified by plate counting. Data were relative to *RBMX2* knockout EBL cells untreated by activators. (C, D) The impact of *M. bovis* BCG and *M. smegmatis* on the adhesion of *RBMX2* knockout EBL cells through plate counting assay. Data were relative to WT EBL cells after BCG and *M. Smegmatis* infection. (E, F) The impact of *M. bovis* BCG and *M. smegmatis* on the invasion of *RBMX2* knockout EBL cells through plate counting assay. Data were relative to WT EBL cells after BCG and *M. Smegmatis* infection. (G, H) The impact of *Salmonella* and *E. coli*, on the adhesion of *RBMX2* knockout EBL cells through plate counting assay. Data were relative to WT EBL cells after *Salmonella* and *E. coli* infection. (K, L) The impact of *Salmonella* and *E. coli* on the invasion of *RBMX2* knockout EBL cells through plate counting assay. Data were relative to WT EBL cells after *Salmonella* and *E. coli* infection. One-way and two-way ANOVA were used to determine the statistical significance of differences between different groups. Ns presents no significance, * presents $p < 0.05$, **presents $p < 0.01$, and *** presents $p < 0.001$ indicate statistically significant differences. Data were representative of at least three independent experiments.

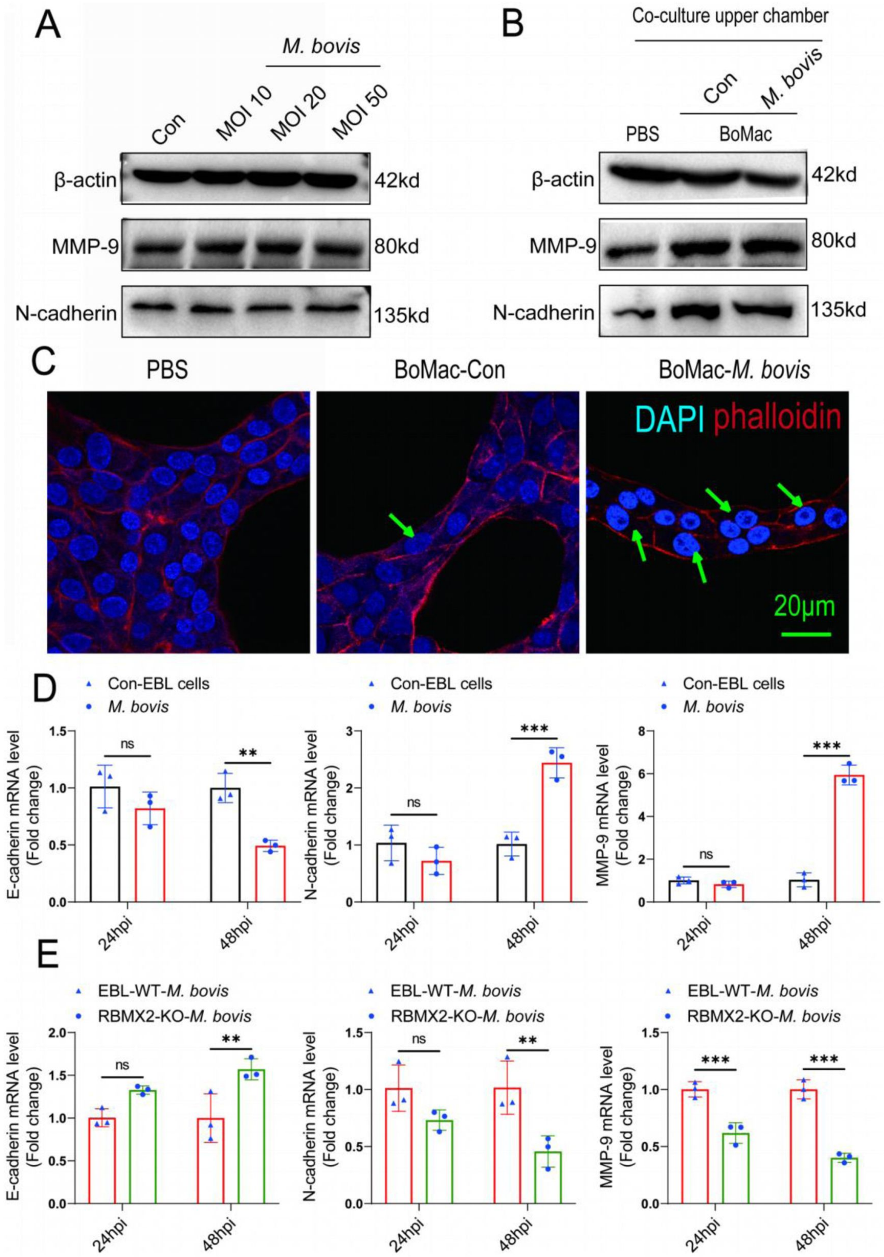

Supplementary Fig 7

RBMX2 facilitates EMT process in EBL cells after *M. bovis*-infected BoMac cells.

(A) WB detection of changes in mesenchymal cell markers (*MMP-9* and *N-cadherin*) after infection of EBL cells with different infection ratios (10, 20, and 50) of *M. bovis*. Data were relative to EBL cells without infection of *M. bovis*. (B) WB detection of the ability of *M. bovis* infection with macrophages (BoMac cells) to induce epithelial (EBL cells) mesenchymal transition. Data were relative to the addition of PBS in the upper chamber of the coculture model. (C) Staining the skeleton of EBL cells in coculture model after *M. bovis* infection using ghost pen cyclic peptides. The cytoskeleton is labeled with red fluorescence, and the nucleus is stained with blue fluorescence. Scale Bar: 20 μm. (D) EMT-related mRNAs (*MMP-9*, *N-cadherin*, and *E-cadherin*) expression was verified in coculture model EBL cells after *M. bovis* infection through RT-qPCR. Data were relative to coculture model EBL cells without *M. bovis* infection. (E) The detection of EMT-related mRNAs (*MMP-9*, *N-cadherin*, and *E-cadherin*) of *RBMX2* knockout EBL cells after *M. bovis-infected* BoMac cells via RT-qPCR. Data were relative to WT EBL cells after *M. bovis-infected* BoMac cells. Two-way ANOVA was used to determine the statistical significance of differences between different groups. Ns presents no significance, **presents $p < 0.01$, and *** presents $p < 0.001$ indicate statistically significant differences. Data were representative of at least three independent experiments.

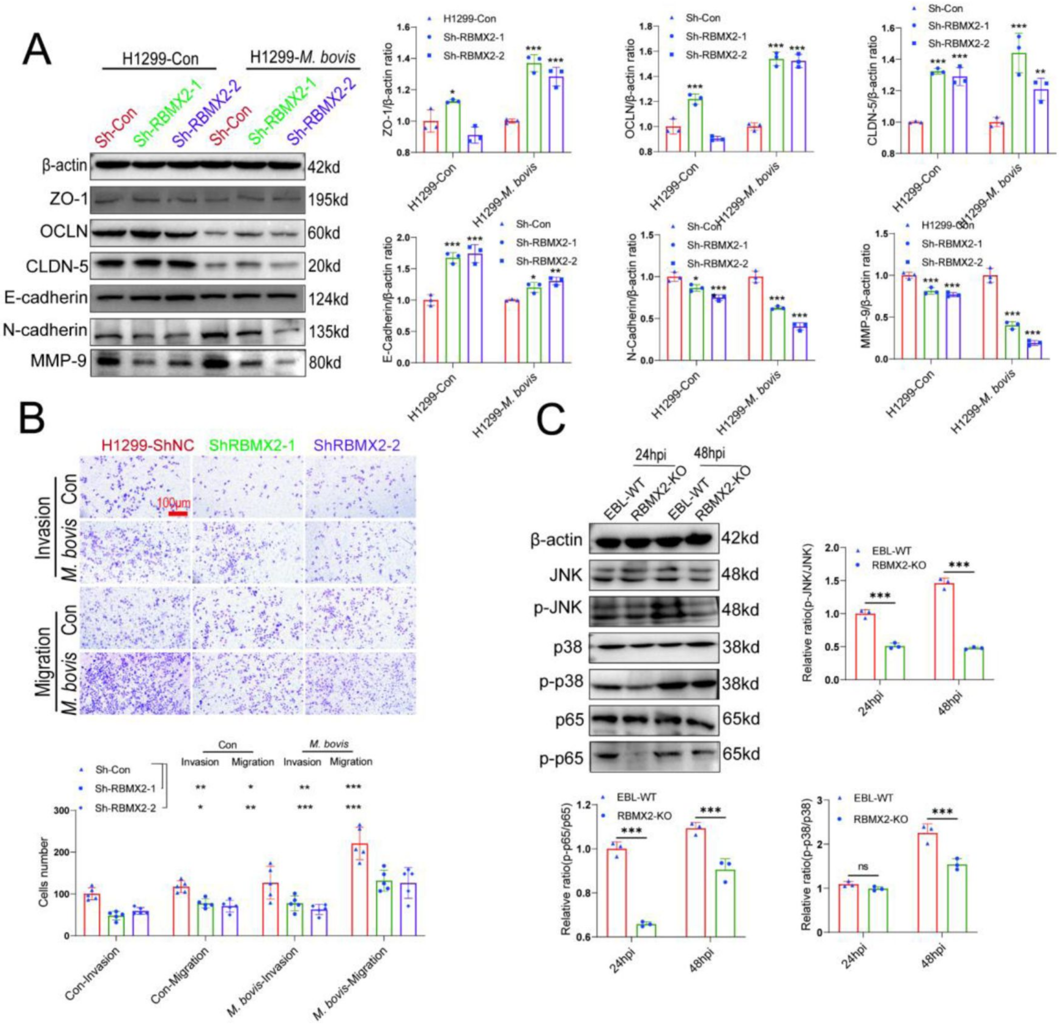

Supplementary Fig 8

RBMX2 facilitates EMT in H1299 cells.

(A) EMT-related proteins expression was verified in H1299 cells after *M. bovis* infection through WB. Data were relative to H1299 Sh-Con cells. (B) The change in the migratory and invasive capabilities of H1299 cells was assessed via Transwell assay. Data were relative to H1299 Sh-Con cells. Scale Bar: 100 μm. (C) Activation of the MAPK pathway-related protein and p65 protein were activated after *RBMX2* knockout and WT EBL cells infected by *M. bovis* in this coculture model via WB. Data were relative to WT EBL cells with *M. bovis* infection. Two-way ANOVA was used to determine the statistical significance of differences between different groups. *$p < 0.05$, **$p < 0.01$, and ***$p < 0.001$ indicate statistically significant differences. Data were representative of at least three independent experiments.

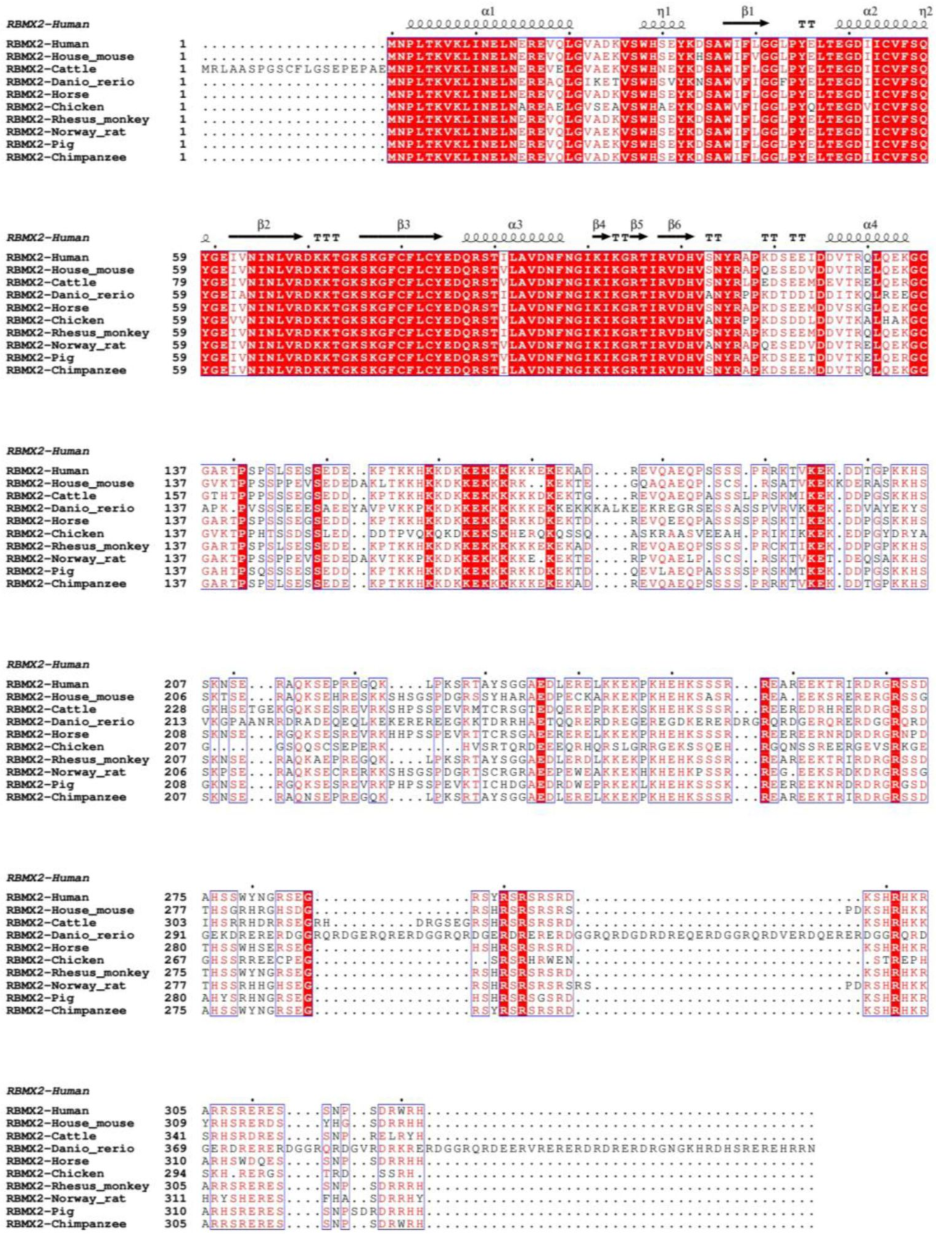

Supplementary Table 1

***RBMX2* exhibits high homology in amino acid sequence alignment across different species**

Acknowledgements

We would like to thank the National Key Laboratory of Agricultural Microbiology Core Facility for assistance in high-throughput microscopy, and we are grateful to Zhe Hu for his support of the sample preparation. This work was supported by the Major projects of agricultural biological breeding in China (2023ZD0405003), the National Natural Science Foundation of China (32072942), China Agriculture Research System of MOF and MARA (CARS-37), National Natural Science Foundation of China (81960772) and Key Project of Inner Mongolia Medical University (YKD2022ZD016).

Additional information

Author Contributions

YC and AG contributed to the conception and design of the study. CW, YP and HY carried out the experiment and wrote sections of the manuscript and made equal contribution. YJ, AK, ZY, KZ, and SX were involved in bacterial and cell research studies. CW, PY, HY, SX, LB, LZ, and CH performed the statistical analysis. CW, AG, and YC wrote the manuscript with all authors providing feedback. All authors contributed to manuscript revision, proof-reading, and approval of the submitted version.

Abbreviations

- *RBMX2*: RNA-binding motif protein X-linked 2
- EBL: embryo bovine lung cells
- BoMac: bovine macrophage cells
- A549: human pulmonary alveolar epithelial cells
- TB: tuberculosis
- *M. bovis*: *Mycobacterium bovis*
- *M. tb*: *Mycobacterium tuberculosis*
- BCG: *Bacillus* Calmette–Guerin
- WOAH: World Organisation for Animal Health
- hpi: hours postinfection
- *M. smegmatis*: *Mycobacterium smegmatis*
- *E. coli*: *Escherichia coli*
- p65: RELA proto-oncogene, NF-kB subunit
- MAPK: mitogen-activated protein kinase
- EMT: epithelial–mesenchymal transition
- PARP: poly ADP-ribose polymerase
- ZO-1: tight junction protein 1
- CLDN-5: claudin 5
- OCLN: occludin
- MMP-9: matrix metallopeptidase 9
- SP-A: surfactant protein A
- GO: Gene Ontology
- KEGG: Kyoto Encyclopedia of Genes and Genomes
- WB: Western blot
- RT-qPCR: real-time quantitative polymerase chain reaction
- IF: immunofluorescence
- ECMy: extracellular matrix

- TCGA: the cancer genome atlas

References

1. WHO (2023) **Global tuberculosis report** Google Scholar

2. Preda M., Tănase B. C., Zob D. L., Gheorghe A. S., Lungulescu C. V., Dumitrescu E. A., Stănculeanu D. L., Manolescu L. S. C., Popescu O., Ibraim E., Mahler B (2023) **The Bidirectional Relationship between Pulmonary Tuberculosis and Lung Cancer** *Int J Environ Res Public Health* **20** Google Scholar

3. Cabrera-Sanchez J., Cuba V., Vega V., Van der Stuyft P., Otero L (2022) **Lung cancer occurrence after an episode of tuberculosis: a systematic review and meta-analysis** *Eur Respir Rev* **31** Google Scholar

4. Suarez-Carmona M., Lesage J., Cataldo D., Gilles C (2017) **EMT and inflammation: inseparable actors of cancer progression** *Mol Oncol* **11**:805–823 Google Scholar

5. Wang C., Jiang Y., Yang Z., Xu H., Khalid A. K., Iftakhar T., Peng Y., Lu L., Zhang L., Bermudez L., Guo A., Chen Y (2024) **Host factor RBMX2 promotes epithelial cell apoptosis by downregulating APAF-1's Retention Intron after Mycobacterium bovis infection** *Front Immunol* **15** Google Scholar

6. Song Y., He S., Ma X., Zhang M., Zhuang J., Wang G., Ye Y., Xia W (2020) **RBMX contributes to hepatocellular carcinoma progression and sorafenib resistance by specifically binding and stabilizing BLACAT1** *Am J Cancer Res* **10**:3644–3665 Google Scholar

7. Schümann F. L., Bauer M., Groß E., Terziev D., Wienke A., Wickenhauser C., Binder M., Weber T (2021) **RBMX Protein Expression in T-Cell Lymphomas Predicts Chemotherapy Response and Prognosis** *Cancers (Basel)* **13** Google Scholar

8. Alors-Pérez E., Blázquez-Encinas R., Moreno-Montilla M. T., García-Vioque V., Jiménez-Vacas J. M., Mafficini A., González-Borja I., Luchini C., Sánchez-Hidalgo J. M., Sánchez-Frías M. E., Pedraza-Arevalo S., Romero-Ruiz A., Lawlor R. T., Viúdez A., Gahete M. D., Scarpa A., Arjona-Sánchez Á., Luque R. M., Ibáñez-Costa A., Castaño J. P (2024) **Spliceosomic dysregulation in pancreatic cancer uncovers splicing factors PRPF8 and RBMX as novel candidate actionable targets** *Mol Oncol* **18**:2524–2540 Google Scholar

9. Wibbe N., Ebnet K (2023) **Cell Adhesion at the Tight Junctions: New Aspects and New Functions** *Cells-Basel* **12** Google Scholar

10. Bhat A. A., Uppada S., Achkar I. W., Hashem S., Yadav S. K., Shanmugakonar M., Al-Naemi H. A., Haris M., Uddin S. (2018) **Tight Junction Proteins and Signaling Pathways in Cancer and Inflammation: A Functional Crosstalk** *Front Physiol* **9**:1942 Google Scholar

11. Zou Y., Xiang Q., Wang J., Peng J., Wei H (2016) **Oregano Essential Oil Improves Intestinal Morphology and Expression of Tight Junction Proteins Associated with Modulation of Selected Intestinal Bacteria and Immune Status in a Pig Model** *Biomed Res Int* **5436738** Google Scholar

12. Edelblum K. L., Turner J. R (2009) **The tight junction in inflammatory disease: communication breakdown** *Curr Opin Pharmacol* **9**:715–20 Google Scholar

13. Bell C. E., Watson A. J (2013) **p38 MAPK regulates cavitation and tight junction function in the mouse blastocyst** *Plos One* **8**:e59528 Google Scholar

14. Kitagawa N., Inai Y., Higuchi Y., Iida H., Inai T (2014) **Inhibition of JNK in HaCaT cells induced tight junction formation with decreased expression of cytokeratin 5, cytokeratin 17 and desmoglein 3** *Histochem Cell Biol* **142**:389–99 Google Scholar

15. Lin X., Zhu Y., Le G (2021) **Tetramethylpyrazine Alleviates Tight Junction Disruption of Bronchial Mucosal Epithelial Cells Caused by Interleukin-17 via Inhibiting Nuclear Factor-κB-p65/Tumor Necrosis Factor-α Signaling Pathway** *J Interferon Cytokine Res* **41**:415–424 Google Scholar

16. Jeong C. H., Seok J. S., Petriello M. C., Han S. G (2017) **Arsenic downregulates tight junction claudin proteins through p38 and NF-κB in intestinal epithelial cell line, HT-29** *Toxicology* **379**:31-39 Google Scholar

17. Singh V., Phukan U. J. (2019) **Interaction of host and Staphylococcus aureus protease-system regulates virulence and pathogenicity** *Med Microbiol Immunol* **208**:585–607 Google Scholar

18. Gu L., Wang H., Guo Y. L., Zen K (2008) **Heparin blocks the adhesion of E. coli O157:H7 to human colonic epithelial cells** *Biochem Biophys Res Commun* **369**:1061–4 Google Scholar

19. Harrandah A. M., Chukkapalli S. S., Bhattacharyya I., Progulske-Fox A., Chan E. K. L (2021) **Fusobacteria modulate oral carcinogenesis and promote cancer progression** *J Oral Microbiol* **13** Google Scholar

20. Li N. S., Xu X. B., Yang H., Wang H., Ouyang Y. B., Zhou Y. A., Peng C., Yuan Z. X., He C., Zeng C. Y., Hong J. B (2021) **Activation of Aquaporin 5 by carcinogenic infection promotes epithelial-mesenchymal transition via the MEK/ERK pathway** *Helicobacter* **26** Google Scholar

21. Bessède E., Dubus P., Mégraud F., Varon C (2015) **, infection and stem cells at the origin of gastric cancer** *Oncogene* **34**:2547–2555 Google Scholar

22. Ferluga J., Yasmin H., Al-Ahdal M. N., Bhakta S., Kishore U (2020) **Natural and trained innate immunity against** *Immunobiology* **225** Google Scholar

23. Strong E. J., Wang J., Ng T. W., Porcelli S. A., Lee S (2022) **Mycobacterium tuberculosis PPE51 Inhibits Autophagy by Suppressing Toll-Like Receptor 2-Dependent Signaling** *Mbio* **13** Google Scholar

24. Vignesh R., Balakrishnan P., Tan H. Y., Yong Y. K., Velu V., Larsson M., Shankar E. M (2023) **Tuberculosis-Associated Immune Reconstitution Inflammatory Syndrome-An Extempore Game of Misfiring with Defense Arsenals** *Pathogens* **12** Google Scholar

25. Certo M., Tsai C. H., Pucino V., Ho P. C., Mauro C (2021) **Lactate modulation of immune responses in inflammatory versus tumour microenvironments** *Nat Rev Immunol* **21**:151–161 Google Scholar

26. Harmon C., O'Farrelly C., Robinson M. W (2020) **The Immune Consequences of Lactate in the Tumor Microenvironment. Tumor Microenvironment: Molecular Players** *Pt A* **1259**:113–124 Google Scholar

27. Rodel H. E., Ferreira I. A. T. M., Ziegler C. G. K., Ganga Y., Bernstein M., Hwa S. H., Nargan K., Lustig G., Kaplan G., Noursadeghi M., Shalek A. K., Steyn A. J. C., Sigal A (2021) **Aggregated Enhances the Inflammatory Response** *Front Microbiol* **12** Google Scholar

28. Park D. W., Moon S. M., Choi H., Kim S. H., Kang H. K., Jung J. H., Han K., Shin D. W., Lee H (2023) **Increased lung cancer risk and associated risk factors in tuberculosis survivors: a Korean population-based study** *Cancer Res* **83** Google Scholar

29. Hu M (2023) **A Case of Multi-Organ Tuberculosis Misdiagnosed as Lung Cancer and a Literature Review** *Cancer Manag Res* **15**:1395–1400 Google Scholar

30. Menakuru S., Dhillon V., Emran J., Khan I., Beirat A., Salih A (2023) **Are Delays In The Diagnosis Of Lung Cancer Due To Patients First Seeking Treatment for Tuberculosis In Rural India?** *J Thorac Oncol* **18**:E23–E23 Google Scholar

31. Liu W., Wang H., Bai F., Ding L., Huang Y., Lu C., Chen S., Li C., Yue X., Liang X., Ma C., Xu L., Gao L (2020) **IL-6 promotes metastasis of non-small-cell lung cancer by up-regulating TIM-4 via NF-κB** *Cell Prolif* **53**:e12776 Google Scholar

32. Shrestha R., Bridle K. R., Crawford D. H. G., Jayachandran A (2020) **TNF-α-mediated epithelial-to-mesenchymal transition regulates expression of immune checkpoint molecules in hepatocellular carcinoma** *Mol Med Rep* **21**:1849–1860 Google Scholar

33. Hao Y., Baker D., Ten Dijke P. (2019) **TGF-β-Mediated Epithelial-Mesenchymal Transition and Cancer Metastasis** *Int J Mol Sci* **20** Google Scholar

34. Xu G., Li Y., Yang J., Zhou X., Yin X., Liu M., Zhao D (2007) **Effect of recombinant Mce4A protein of Mycobacterium bovis on expression of TNF-alpha, iNOS** *IL-6, and IL-12 in bovine alveolar macrophages. Mol Cell Biochem* **302**:1-7 Google Scholar

35. Na T. Y., Schecterson L., Mendonsa A. M., Gumbiner B. M (2020) **The functional activity of E-cadherin controls tumor cell metastasis at multiple steps** *P Natl Acad Sci USA* **117**:5931–5937 Google Scholar

36. Fedele M., Sgarra R., Battista S., Cerchia L., Manfioletti G (2022) **The Epithelial-Mesenchymal Transition at the Crossroads between Metabolism and Tumor Progression** *Int J Mol Sci* **23** Google Scholar

37. Alqurashi Y. E., Al-Hetty H. R. A. K., Ramaiah P., Fazaa A. H., Jalil A. T., Alsaikhan F., Gupta J., Ramírez-Coronel A. A., Tayyib N. A., Peng H (2023) **Harnessing function of EMT in hepatocellular carcinoma: From biological view to nanotechnological standpoint** *Environ Res* **227** Google Scholar

38. Mirzaei S., Saghari S., Bassiri F., Raesi R., Zarrabi A., Hushmandi K., Sethi G., Tergaonkar V (2022) **NF-κB as a regulator of cancer metastasis and therapy response: A focus on epithelial-mesenchymal transition** *J Cell Physiol* **237**:2770–2795 Google Scholar

39. O'Leary K., Shia A., Schmid P (2018) **Epigenetic Regulation of EMT in Non-Small Cell Lung Cancer** *Curr Cancer Drug Tar* **18**:89–96 Google Scholar

40. Stefani C., Miricescu D., Stanescu-Spinu I. I., Nica R. I., Greabu M., Totan A. R., Jinga M., Factors Growth (2021) **PI3K/AKT/mTOR and MAPK Signaling Pathways in Colorectal Cancer Pathogenesis: Where Are We Now?** *Int J Mol Sci* **22** Google Scholar

41. Kim B. K., Kim D. M., Park H., Kim S. K., Hwang M. A., Lee J., Kang M. J., Byun J. E., Im J. Y., Kang M., Park K. C., Yeom Y. I., Kim S. Y., Jung H., Kweon D. H., Cheong J. H., Won M. (2022) **Synaptotagmin 11 scaffolds MKK7-JNK signaling process to promote stem-like molecular subtype gastric cancer oncogenesis** *J Exp Clin Canc Res* **41** Google Scholar

42. Gonzalez-Avila G., Sommer B., García-Hernández A. A., Ramos C (2020) **Matrix Metalloproteinases' Role in Tumor Microenvironment** *Tumor Microenvironment: Extracellular Matrix Components - Pt A* **1245**:97–131 Google Scholar

43. Cox T. R (2021) **The matrix in cancer** *Nat Rev Cancer* **21**:217–238 Google Scholar

44. Kwaan H. C., Lindholm P. F. (2019) **Fibrin and Fibrinolysis in Cancer** *Semin Thromb Hemost* **45**:413–422 Google Scholar

45. Mego M., Karaba M., Minarik G., Benca J., Sedlácková T., Tothova L., Vlkova B., Cierna Z., Janega P., Luha J., Gronesova P., Pindak D., Fridrichova I., Celec P., Reuben J. M., Cristofanilli M., Mardiak J (2015) **Relationship between Circulating Tumor Cells, Blood Coagulation, and Urokinase-Plasminogen-Activator System in Early Breast Cancer Patients** *Breast J* **21**:155–160 Google Scholar

46. Kim J. H (2020) **Interleukin-8 in the Tumor Immune Niche: Lessons from Comparative Oncology. Tumor Microenvironment: The Role of Interleukins** *Pt A* **1240**:25–33 Google Scholar

47. Zuo J. H., Zhu W., Li M. Y., Li X. H., Yi H., Zeng G. Q., Wan X. X., He Q. Y., Li J. H., Qu J. Q., Chen Y., Xiao Z. Q (2011) **Activation of EGFR promotes squamous carcinoma SCC10A cell migration and invasion via inducing EMT-like phenotype change and MMP-9-mediated degradation of E-cadherin** *J Cell Biochem* **112**:2508–17 Google Scholar

48. Peng W., Jiang J., Fu J., Duan H., Wang J., Duan C (2023) **lncRNA GMDS-AS1 restrains lung adenocarcinoma progression via recruiting TAF15 protein to stabilize SIRT1 mRNA** *Epigenomics* **15**:417–434 Google Scholar

49. Reis A. C., Cunha M. V (2021) **The open pan-genome architecture and virulence landscape of Mycobacterium bovis** *Microb Genomics* **7** Google Scholar

50. Fan Y. L., Wu J. B., Cheng X. W., Zhang F. Z., Feng L. S (2018) **Fluoroquinolone derivatives and their anti-tubercular activities** *Eur J Med Chem* **146**:554–563 Google Scholar

51. Borkowska D. I., Napiórkowska A. M., Brzezinska S. A., Kozinska M., Zabost A. T., Augustynowicz-Kopec E. M (2017) **From Latent Tuberculosis Infection to Tuberculosis. News in Diagnostics (QuantiFERON-Plus)** *Pol J Microbiol* **66**:5–8 Google Scholar

52. Rastogi N., Zarin S., Alam A., Konduru G. V., Manjunath P., Mishra A., Kumar S., Nagarajaram H. A., Hasnain S. E., Ehtesham N. Z. (2023) **Structural and Biophysical properties of therapeutically important proteins Rv1509 and Rv2231A of Mycobacterium tuberculosis** *Int J Biol Macromol* **245** Google Scholar

53. Corleis B., Dorhoi A (2020) **Early dynamics of innate immunity during pulmonary tuberculosis** *Immunol Lett* **221**:56–60 Google Scholar

54. Abebe F (2021) **Crosstalk between Mycobacterium tuberculosis and the host cell** *Clin Exp Immunol* **204**:32–40 Google Scholar

55. Reuschl A. K., Edwards M. R., Parker R., Connell D. W., Hoang L., Halliday A., Jarvis H., Siddiqui N., Wright C., Bremang S., Newton S. M., Beverley P., Shattock R. J., Kon M., Lalvanl A (2017) **Innate activation of human primary epithelial cells broadens the host response to in the airways** *Plos Pathog* **13** Google Scholar

56. Dorhoi A., Kaufmann S. H. E (2014) **Perspectives on host adaptation in response to: Modulation of inflammation** *Semin Immunol* **26**:533–542 Google Scholar

57. Rajararna M. V. S., Ni B., Dodd C. E., Schlesinger L. S (2014) **Macrophage immunoregulatory pathways in tuberculosis** *Semin Immunol* **26**:471–485 Google Scholar

58. D'Agnillo F., Walters K. A., Xiao Y. L., Sheng Z. M., Scherler K., Park J., Gygli S., Rosas L. A., Sadtler K., Kalish H., Blatti C. A., Zhu R. Q., Gatzke L., Bushell C., Memoli M. J., O'Day S. J., Fischer T. D., Hammond T. C., Lee R. C., Cash J. C., Powers M. E., O'Keefe G. E., Butnor K. J., Rapkiewicz A. V., Travis W. D., Layne S. P., Kash J. C., Taubenberger J. K. (2021) **Lung epithelial and endothelial damage, loss of tissue repair, inhibition of fibrinolysis, and cellular senescence in fatal COVID-19** *Sci Transl Med* **13** Google Scholar

59. Barros B. C. S. C., Almeida B. R., Barros D. T. L., Toledo M. S., Suzuki E., Cells Respiratory Epithelial (2022) **More Than Just a Physical Barrier to Fungal Infections** *J Fungi* **8** Google Scholar

60. Hu Y., Mu H. S., Deng Z. P (2023) **RBM14 as a novel epigenetic-activated tumor oncogene is implicated in the reprogramming of glycolysis in lung cancer** *World J Surg Oncol* **21** Google Scholar

61. Buckley A., Turner J. R (2018) **Cell Biology of Tight Junction Barrier Regulation and Mucosal Disease** *Csh Perspect Biol* **10** Google Scholar

62. Rastegar D. A., Tabar M. S., Alikhani M., Parsamatin P., Samani F. S., Sabbaghian M., Gilani M. A. S., Ahadi A. M., Meybodi A. M., Piryaei A., Ansari-Pour N., Gourabi H., Baharvand H., Salekdeh G. H (2015) **Isoform-Level Gene Expression Profiles of Human Y Chromosome Azoospermia Factor Genes and Their X Chromosome Paralogs in the Testicular Tissue of Non-Obstructive Azoospermia Patients** *J Proteome Res* **14**:3595–3605 Google Scholar

63. Zhu Y. C., Zheng M. H., Song D. L., Ye L., Wang X. D (2015) **Global comparison of chromosome X genes of pulmonary telocytes with mesenchymal stem cells, fibroblasts, alveolar type II cells, airway epithelial cells, and lymphocytes** *J Transl Med* **13** Google Scholar

64. Zhang X. T., Zhang J. R., Zhao W., Dong X., Xin P., Liu X., Li X. J., Jing Z. F., Zhang Z., Kong C. Z., Yu X. Y (2021) **Long non-coding RNA LINC02446 suppresses the proliferation and metastasis of bladder cancer cells by binding with EIF3G and regulating the mTOR signalling pathway** *Cancer Gene Ther* **28**:1376–1389 Google Scholar

65. Savagner P (2015) **Epithelial-Mesenchymal Transitions: From Cell Plasticity to Concept Elasticity** *Curr Top Dev Biol* **112**:273–300 Google Scholar

eLife

66. Kyuno D., Takasawa A., Kikuchi S., Takemasa I., Osanai M., Kojima T (2021) **Role of tight junctions in the epithelial-to-mesenchymal transition of cancer cells** *Bba-Biomembranes* **1863** Google Scholar

67. Hashimoto I., Oshima T. (2022) **Claudins and Gastric Cancer: An Overview** *Cancers* **14** Google Scholar

68. Malfertheiner P., Camargo M. C., El-Omar E., Liou J. M., Peek R., Schulz C., Smith S. I., Suerbaum S. (2023) **Helicobacter pylori infection** *Nat Rev Dis Primers* **9** Google Scholar

69. de Brito B. B., da Silva F. A. F., Soares A. S., Pereira V. A., Santos M. L. C., Sampaio M. M., Neves P. H. M., de Melo F. F (2019) **Pathogenesis and clinical management of gastric infection** *World J Gastroentero* **25**:5578–5589 Google Scholar

70. Ho J. C. M., Leung C. C (2018) **Management of co-existent tuberculosis and lung cancer** *Lung Cancer* **122**:83–87 Google Scholar

71. Christopoulos A., Saif M. W., Sarris E. G., Syrigos K. N (2014) **Epidemiology of active tuberculosis in lung cancer patients: a systematic review** *Clin Respir J* **8**:375–381 Google Scholar

72. Nalbandian A., Yan B. S., Pichugin A., Bronson R. T., Kramnik I (2009) **Lung carcinogenesis induced by chronic tuberculosis infection: the experimental model and genetic control** *Oncogene* **28**:1928–1938 Google Scholar

73. Holla S., Ghorpade D. S., Singh V., Bansal K., Balaji K. N (2014) **BCG promotes tumor cell survival from tumor necrosis factor-α-induced apoptosis** *Mol Cancer* **13** Google Scholar

74. Gupta P. K., Tripathi D., Kulkarni S., Rajan M. G. R (2016) **H37Rv infected THP-1 cells induce epithelial mesenchymal transition (EMT) in lung adenocarcinoma epithelial cell line (A549)** *Cell Immunol* **300**:33–40 Google Scholar

75. Leung C. Y., Huang H. L., Rahman M. M., Nomura S., Abe S. K., Saito E., Shibuya K (2020) **Cancer incidence attributable to tuberculosis in 2015: global, regional, and national estimates** *Bmc Cancer* **20** Google Scholar

76. De La Barrera S., Alemán M., Musella R., Schierloh P., Pasquinelli V., García V., Abbate E., Sasiain M. D (2004) **IL-10 down-regulates costimulatory molecules on-pulsed macrophages and impairs the lytic activity of CD4 and CD8 CTL in tuberculosis patients** *Clin Exp Immunol* **138**:128–138 Google Scholar

77. Chen X., Huang J., Zhu H. M., Guo Y. P., Khan F. A., Menghwar H., Zhao G., Guo A. Z (2018) **P27 (MBOV_RS03440) is a novel fibronectin binding adhesin of Mycoplasma bovis** *Int J Med Microbiol* **308**:848–857 Google Scholar

78. Zhao G., Zhu X. F., Zhang H., Chen Y. Y., Schieck E., Hu C. M., Chen H. C., Guo A (2021) **Novel Secreted Protein of MbovP280 Induces Macrophage Apoptosis Through CRYAB** *Front Immunol* **12** Google Scholar

79. Li T., He J., Cao H., Zhang Y., Chen J., Xiao Y., Huang S. Y (2024) **All-atom RNA structure determination from cryo-EM maps** *Nat Biotechnol* Google Scholar

Author information

Chao Wang
The National Key Laboratory of Agricultural Microbiology, College of Veterinary Medicine, Huazhong Agricultural University, Wuhan, China, National Animal Tuberculosis Para-Reference Laboratory (Wuhan) of Ministry of Agriculture and Rural Affairs, Huazhong Agricultural University, Wuhan, China, Center for Infectious Disease Research, School of Medicine, Westlake University, Hangzhou, China

Yongchong Peng
The National Key Laboratory of Agricultural Microbiology, College of Veterinary Medicine, Huazhong Agricultural University, Wuhan, China, National Animal Tuberculosis Para-Reference Laboratory (Wuhan) of Ministry of Agriculture and Rural Affairs, Huazhong Agricultural University, Wuhan, China

Hongxin Yang
Oncology Collaborative Innovation Center, Inner Mongolia Medical University, Hohhot, China, Oncology Collaborative Innovation Center, Inner Mongolia Medical University, Hohhot, China

Yanzhu Jiang
The National Key Laboratory of Agricultural Microbiology, College of Veterinary Medicine, Huazhong Agricultural University, Wuhan, China, National Animal Tuberculosis Para-Reference Laboratory (Wuhan) of Ministry of Agriculture and Rural Affairs, Huazhong Agricultural University, Wuhan, China

Abdul Karim Khalid
The National Key Laboratory of Agricultural Microbiology, College of Veterinary Medicine, Huazhong Agricultural University, Wuhan, China

Kailun Zhang
The National Key Laboratory of Agricultural Microbiology, College of Veterinary Medicine, Huazhong Agricultural University, Wuhan, China, National Animal Tuberculosis Para-Reference Laboratory (Wuhan) of Ministry of Agriculture and Rural Affairs, Huazhong Agricultural University, Wuhan, China

Shengsong Xie
The National Key Laboratory of Agricultural Microbiology, College of Veterinary Medicine, Huazhong Agricultural University, Wuhan, China

Luiz Bermudez
Department of Biomedical Sciences, College of Veterinary Medicine, Oregon State University, Corvallis, United States

Yong Yang
Department of Surgical Oncology, People’s Hospital of Inner Mongolia Autonomous Region, Hohhot, China

Lei Zhang
The National Key Laboratory of Agricultural Microbiology, College of Veterinary Medicine, Huazhong Agricultural University, Wuhan, China, National Animal Tuberculosis Para-Reference Laboratory (Wuhan) of Ministry of Agriculture and Rural Affairs, Huazhong Agricultural University, Wuhan, China

Huanchun Chen
The National Key Laboratory of Agricultural Microbiology, College of Veterinary Medicine, Huazhong Agricultural University, Wuhan, China

Aizhen Guo
The National Key Laboratory of Agricultural Microbiology, College of Veterinary Medicine, Huazhong Agricultural University, Wuhan, China, National Animal Tuberculosis Para-Reference Laboratory (Wuhan) of Ministry of Agriculture and Rural Affairs, Huazhong Agricultural University, Wuhan, China, Hubei Hongshan Laboratory, Huazhong Agricultural University, Wuhan, China

For correspondence: aizhen@mail.hzau.edu.cn

Yingyu Chen
The National Key Laboratory of Agricultural Microbiology, College of Veterinary Medicine, Huazhong Agricultural University, Wuhan, China, National Animal Tuberculosis Para-Reference Laboratory (Wuhan) of Ministry of Agriculture and Rural Affairs, Huazhong Agricultural University, Wuhan, China
ORCID iD: 0000-0002-1200-5314

For correspondence: chenyingyu@mail.hzau.edu.cn

Editors

Reviewing Editor
Warren Andrew Andayi
Murang'a University of Technology, Murang'a, Kenya

Senior Editor
Bavesh Kana
University of the Witwatersrand, Johannesburg, South Africa

Reviewer #1 (Public review):

Summary:

This manuscript presents a compelling study identifying RBMX2 as a novel host factor upregulated during Mycobacterium bovis infection.

The study demonstrates that RBMX2 plays a role in:

(1) Facilitating M. bovis adhesion, invasion, and survival in epithelial cells.

(2) Disrupting tight junctions and promoting EMT.

(3) Contributing to inflammatory responses and possibly predisposing infected tissue to lung cancer development.

By using a combination of CRISPR-Cas9 library screening, multi-omics, coculture models, and bioinformatics, the authors establish a detailed mechanistic link between M. bovis infection and cancer-related EMT through the p65/MMP-9 signaling axis. Identification of RBMX2 as a bridge between TB infection and EMT is novel.

Strengths:

This topic and data are both novel and significant, expanding the understanding of transcriptomic diversity beyond RBM2 in M. bovis responsive functions.

Weaknesses:

(1) The abstract and introduction sometimes suggest RBMX2 has protective anti-TB functions, yet results show it facilitates pathogen adhesion and survival. The authors need to rephrase claims to avoid contradiction.

(2) While p65/MMP-9 is convincingly implicated, the role of MAPK/p38 and JNK is less clearly resolved.

(3) Metabolomics results are interesting but not integrated deeply into the main EMT narrative.

(4) A key finding and starting point of this study is the upregulation of RBMX2 upon M. bovis infection. However, the authors have only assessed RBMX2 expression at the mRNA level following infection with M. bovis and BCG. To strengthen this conclusion, it is essential to validate RBMX2 expression at the protein level through techniques such as Western blotting or immunofluorescence. This would significantly enhance the credibility and impact of the study's foundational observation.

(5) The manuscript would benefit from a more in-depth discussion of the relationship between tuberculosis (TB) and lung cancer. While the study provides experimental evidence suggesting a link via EMT induction, integrating current literature on the epidemiological and mechanistic connections between chronic TB infection and lung tumorigenesis would provide important context and reinforce the translational relevance of the findings.

https://doi.org/10.7554/eLife.107132.1.sa3

Reviewer #2 (Public review):

Summary:

I am not familiar with cancer biology, so my review mainly focuses on the infection part of the manuscript. Wang et al identified an RNA-binding protein RBMX2 that links the Mycobacterium bovis infection to the epithelial-Mesenchymal transition and lung cancer progression. Upon mycobacterium infection, the expression of RBMX2 was moderately increased in multiple bovine and human cell lines, as well as bovine lung and liver tissues. Using global approaches, including RNA-seq and proteomics, the authors identified differential gene expression caused by the RBMX2 knockout during M. bovis infection. Knockout of RBMX2 led to significant upregulations of tight-junction related genes such as CLDN-5, OCLN, ZO-1, whereas M. bovis infection affects the integrity of epithelial cell tight junctions and inflammatory responses. This study establishes that RBMX2 is an important host factor that modulates the infection process of M. bovis.

Strengths:

(1) This study tested multiple types of bovine and human cells, including macrophages, epithelial cells, and clinical tissues at multiple timepoints, and firmly confirmed the induced expression of RBMX2 upon M. bovis infection.

(2) The authors have generated the monoclonal RBMX2 knockout cell lines and comprehensively characterized the RBMX2-dependent gene expression changes using a combination of global omics approaches. The study has validated the impact of RBMX2 knockout on the tight-junction pathway and on the M. bovis infection, establishing RBMX2 as a crucial host factor.

Weaknesses:

(1) The RBMX2 was only moderately induced (less than 2-fold) upon M. bovis infection, arguing its contribution may be small. Its value as a therapeutic target is not justified. How RBMX2 was activated by M. bovis infection was unclear.

(2) Although multiple time points have been included in the study, most analyses lack temporal resolution. It is difficult to appreciate the impact/consequence of M. bovis infection on the analyzed pathways and processes.

https://doi.org/10.7554/eLife.107132.1.sa2

Reviewer #3 (Public review):

Summary:

This study investigates the role of the host protein RBMX2 in regulating the response to Mycobacterium bovis infection and its connection to epithelial-mesenchymal transition (EMT), a key pathway in cancer progression. Using bovine and human cell models, the authors have wisely shown that RBMX2 expression is upregulated following M. bovis infection and promotes bacterial adhesion, invasion, and survival by disrupting epithelial tight junctions via the p65/MMP-9 signaling pathway. They also demonstrate that RBMX2 facilitates EMT and is overexpressed in human lung cancers, suggesting a potential link between chronic infection and tumor progression. The study highlights RBMX2 as a novel host factor that could serve as a therapeutic target for both TB pathogenesis and infection-related cancer risk.

Strengths:

The major strengths lie in its multi-omics integration (transcriptomics, proteomics, metabolomics) to map RBMX2's impact on host pathways, combined with rigorous functional assays (knockout/knockdown, adhesion/invasion, barrier tests) that establish causality through the p65/MMP-9 axis. Validation across bovine and human cell models and in clinical tissue samples enhances translational relevance. Finally, identifying RBMX2 as a novel regulator linking mycobacterial infection to EMT and cancer progression opens exciting therapeutic avenues.

Weaknesses:

Although it's a solid study, there are a few weaknesses noted below.

(1) In the transcriptomics analysis, the authors performed (GO/KEGG) to explore biological functions. Did they perform the search locally or globally? If the search was performed with a global reference, then I would recommend doing a local search. That would give more relevant results. What is the logic behind highlighting some of the enriched pathways (in red), and how are they relevant to the current study?

(2) While the authors show that RBMX2 expression correlates with EMT-related gene expression and barrier dysfunction, the evidence for direct association remains limited in this study. How does RBMX2 activate p65? Does it bind directly to p65 or modulate any upstream kinases? Could ChIP-seq or CLIP-seq provide further evidence for direct RNA or DNA targets of RBMX2 that drive EMT or NF-κB signaling?

(3) The manuscript suggests that RBMX2 enhances adhesion/invasion of several bacterial species (e.g., E. coli, Salmonella), not just M. bovis. This raises questions about the specificity of RBMX2's role in Mycobacterium-specific pathogenesis. Is RBMX2 a general epithelial barrier regulator or does it exhibit preferential effects in mycobacterial infection contexts? How does this generality affect its potential as a TB-specific therapeutic target?

(4) The quality of the figures is very poor. High-resolution images should be provided.

(5) The methods are not very descriptive, particularly the omics section.

(6) The manuscript is too dense, with extensive multi-omics data (transcriptomics, proteomics, metabolomics) but relatively little mechanistic integration. The authors should have focused on the key mechanistic pathways in the figures. Improving the narratives in the Results and Discussion section could help readers follow the logic of the experimental design and conclusions.

https://doi.org/10.7554/eLife.107132.1.sa1

Author response:

> ***Public Reviews:***
>
> ***Reviewer #1 (Public review):***
>
> *Summary:*
>
> *This manuscript presents a compelling study identifying RBMX2 as a novel host factor upregulated during Mycobacterium bovis infection.*
>
> *The study demonstrates that RBMX2 plays a role in:*
>
> *(1) Facilitating M. bovis adhesion, invasion, and survival in epithelial cells.*
>
> *(2) Disrupting tight junctions and promoting EMT.*
>
> *(3) Contributing to inflammatory responses and possibly predisposing infected tissue to lung cancer development.*
>
> *By using a combination of CRISPR-Cas9 library screening, multi-omics, coculture models, and bioinformatics, the authors establish a detailed mechanistic link between M. bovis infection and cancer-related EMT through the p65/MMP-9 signaling axis. Identification of RBMX2 as a bridge between TB infection and EMT is novel.*
>
> *Strengths:*
>
> *This topic and data are both novel and significant, expanding the understanding of transcriptomic diversity beyond RBM2 in M. bovis responsive functions.*
>
> *Weaknesses:*

> *(1) The abstract and introduction sometimes suggest RBMX2 has protective anti-TB functions, yet results show it facilitates pathogen adhesion and survival. The authors need to rephrase claims to avoid contradiction.*

We sincerely appreciate the reviewer's valuable feedback regarding the need to clarify RBMX2's role throughout the manuscript. We have carefully revised the text to ensure consistent messaging about RBMX2's function in promoting M. bovis infection. Below we detail the specific modifications made:

(1) Introduction Revisions:

Changed "The objective of this study was to elucidate the correlation between host genes and the susceptibility of M.bovis infection" to "The objective of this study was to identify host factors that promote susceptibility to M.bovis infection"

Revised "RBMX2 polyclonal and monoclonal cell lines exhibited favorable phenotypes" to "RBMX2 knockout cell lines showed reduced bacterial survival"

Replaced "The immune regulatory mechanism of RBMX2" with "The role of RBMX2 in facilitating M.bovis immune evasion"

(2) Results Revisions:

Modified "RBMX2 fails to affect cell morphology and the ability to proliferate and promotes M.bovis infection" to "RBMX2 does not alter cell viability but significantly enhances M.bovis infection"

Strengthened conclusion in Figure 4: "RBMX2 actively disrupts tight junctions to facilitate bacterial invasion"

(3) Discussion Revisions:

Revised screening description: "We screened host factors affecting M.bovis susceptibility and identified RBMX2 as a key promoter of infection"

Strengthened concluding statement: "In summary, RBMX2 drives TB pathogenesis by compromising epithelial barriers and inducing EMT"

These targeted revisions ensure that:

All sections consistently present RBMX2 as promoting infection; the language aligns with our experimental finding; potential protective interpretations have been eliminated. We believe these modifications have successfully addressed the reviewer's concern while maintaining the manuscript's original structure and scientific content. We appreciate the opportunity to improve our manuscript and thank the reviewer for this constructive suggestion.

(2) >While p65/MMP-9 is convincingly implicated, the role of MAPK/p38 and JNK is less clearly resolved.

We sincerely appreciate the reviewer's insightful comment regarding the roles of MAPK/p38 and JNK in our study. Our experimental data clearly demonstrated that RBMX2 knockout significantly reduced phosphorylation levels of p65, p38, and JNK (Fig. 5A), indicating potential involvement of all three pathways in RBMX2-mediated regulation.

Through systematic functional validation, we obtained several important findings:

In pathway inhibition experiments, p65 activation (PMA treatment) showed the most dramatic effects on both tight junction disruption (ZO-1, OCLN reduction) and EMT marker regulation (E-cadherin downregulation, N-cadherin upregulation);

p38 activation (ML141 treatment) exhibited moderate effects on these processes;

JNK activation (Anisomycin treatment) displayed minimal impact.

Most conclusively, siRNA-mediated silencing of p65 alone was sufficient to:

Restore epithelial barrier function

Reverse EMT marker expression

Reduce bacterial adhesion and invasion

These results establish a clear hierarchy in pathway importance: p65 serves as the primary mediator of RBMX2's effects, while p38 plays a secondary role and JNK appears non-essential under our experimental conditions. We have now clarified this relationship in the revised Discussion section to strengthen this conclusion.

This refined understanding of pathway hierarchy provides important mechanistic insights while maintaining consistency with all our experimental data. We thank the reviewer for this valuable suggestion that helped improve our manuscript.

> *(3) Metabolomics results are interesting but not integrated deeply into the main EMT narrative.*

Thank you for this constructive suggestion. In this article, we detected the metabolome of RBMX2 knockout and wild-type cells after Mycobacterium bovis infection, which mainly served as supporting evidence for our EMT model. However, we did not conduct an in-depth discussion of these findings. We have now added a detailed discussion of this section to further support our EMT model.

ADD:Meanwhile, metabolic pathways enriched after RBMX2 deletion, such as nucleotide metabolism, nucleotide sugar synthesis, and pentose interconversion, primarily support cell proliferation and migration during EMT by providing energy precursors, regulating glycosylation modifications, and maintaining redox balance; cofactor synthesis and amino sugar metabolism participate in EMT regulation through influencing metabolic remodeling and extracellular matrix interactions; chemokine and cGMP-PKG signaling pathways may further mediate inflammatory responses and cytoskeletal rearrangements, collectively promoting the EMT process.

> *(4) A key finding and starting point of this study is the upregulation of RBMX2 upon M. bovis infection. However, the authors have only assessed RBMX2 expression at the mRNA level following infection with M. bovis and BCG. To strengthen this conclusion, it is essential to validate RBMX2 expression at the protein level through techniques such as Western blotting or immunofluorescence. This would significantly enhance the credibility and impact of the study's foundational observation.*

Thank you for your comment. We have supplemented the experiments in this part and found that Mycobacterium bovis infection can significantly enhance the expression level of RBMX2 protein.

> *(5) The manuscript would benefit from a more in-depth discussion of the relationship between tuberculosis (TB) and lung cancer. While the study provides experimental evidence suggesting a link via EMT induction, integrating current literature on the epidemiological and mechanistic connections between chronic TB infection and lung*

> *tumorigenesis would provide important context and reinforce the translational relevance of the findings.*

We sincerely appreciate the valuable comments from the reviewer. We fully agree with your suggestion to further explore the relationship between tuberculosis (TB) and lung cancer. In the revised manuscript, we will add a new paragraph in the Discussion section to systematically integrate the current literature on the epidemiological and mechanistic links between chronic tuberculosis infection and lung cancer development, including the potential bridging roles of chronic inflammation, tissue damage repair, immune microenvironment remodeling, and the epithelial-mesenchymal transition (EMT) pathway. This addition will help more comprehensively interpret the clinical implications of the observed EMT activation in the context of our study, thereby enhancing the biological plausibility and clinical translational value of our findings.

ADD:There is growing epidemiological evidence suggesting that chronic TB infection represents a potential risk factor for the development of lung cancer. Studies have shown that individuals with a history of TB exhibit a significantly increased risk of lung cancer, particularly in areas of the lung with pre-existing fibrotic scars, indicating that chronic inflammation, tissue repair, and immune microenvironment remodeling may collectively contribute to malignant transformation 74. Moreover, EMT not only endows epithelial cells with mesenchymal features that enhance migratory and invasive capacity but is also associated with the acquisition of cancer stem cell-like properties and therapeutic resistance 75. Therefore, EMT may serve as a crucial molecular link connecting chronic TB infection with the malignant transformation of lung epithelial cells, warranting further investigation in the intersection of infection and tumorigenesis.

> ***Reviewer #2 (Public review):***
>
> *Summary:*
>
> *I am not familiar with cancer biology, so my review mainly focuses on the infection part of the manuscript. Wang et al identified an RNA-binding protein RBMX2 that links the Mycobacterium bovis infection to the epithelial-Mesenchymal transition and lung cancer progression. Upon mycobacterium infection, the expression of RBMX2 was moderately increased in multiple bovine and human cell lines, as well as bovine lung and liver tissues. Using global approaches, including RNA-seq and proteomics, the authors identified differential gene expression caused by the RBMX2 knockout during M. bovis infection. Knockout of RBMX2 led to significant upregulations of tight-junction related genes such as CLDN-5, OCLN, ZO-1, whereas M. bovis infection affects the integrity of epithelial cell tight junctions and inflammatory responses. This study establishes that RBMX2 is an important host factor that modulates the infection process of M. bovis.*
>
> *Strengths:*
>
> *(1) This study tested multiple types of bovine and human cells, including macrophages, epithelial cells, and clinical tissues at multiple timepoints, and firmly confirmed the induced expression of RBMX2 upon M. bovis infection.*
>
> *(2) The authors have generated the monoclonal RBMX2 knockout cell lines and comprehensively characterized the RBMX2-dependent gene expression changes using a combination of global omics approaches. The study has validated the impact of RBMX2 knockout on the tight-junction pathway and on the M. bovis infection, establishing RBMX2 as a crucial host factor.*
>
> *Weaknesses:*

> *(1) The RBMX2 was only moderately induced (less than 2-fold) upon M. bovis infection, arguing its contribution may be small. Its value as a therapeutic target is not justified. How RBMX2 was activated by M. bovis infection was unclear.*

Thank you for your valuable and constructive comments. In this study, we primarily utilized the CRISPR whole-genome screening approach to identify key factors involved in bovine tuberculosis infection. Through four rounds of screening using a whole-genome knockout cell line of bovine lung epithelial cells infected with Mycobacterium bovis, we identified RBMX2 as a critical factor.

Although the transcriptional level change of RBMX2 was less than two-fold, following the suggestion of Reviewer 1, we examined its expression at the protein level, where the change was more pronounced, and we have added these results to the manuscript.

Regarding the mechanism by which RBMX2 is activated upon M. bovis infection, we previously screened for interacting proteins using a Mycobacterium tuberculosis secreted and membrane protein library, but unfortunately, we did not identify any direct interacting proteins from M. tuberculosis (https://doi.org/10.1093/nar/gkx1173).

> *(2) Although multiple time points have been included in the study, most analyses lack temporal resolution. It is difficult to appreciate the impact/consequence of M. bovis infection on the analyzed pathways and processes.*

We appreciate the valuable comments from the reviewers. Although our study included multiple time points post-infection, in our experimental design we focused on different biological processes and phenotypes at distinct time points:

During the early phase (e.g., 2 hours post-infection), we focused on barrier phenotypes; during the intermediate phase (e.g., 24 hours post-infection), we concentrated more on pathway activation and EMT phenotypes;

And during the later phase (e.g., 48–72 hours post-infection), we focused more on cell death phenotypes, which were validated in another FII article (https://doi.org/10.3389/fimmu.2024.1431207).

We also examined the impact of varying infection durations on RBMX2 knockout EBL cellular lines via GO analysis. At 0 hpi, genes were primarily related to the pathways of cell junctions, extracellular regions, and cell junction organization. At 24 hpi, genes were mainly associated with pathways of the basement membrane, cell adhesion, integrin binding and cell migration By 48 hpi, genes were annotated into epithelial cell differentiation and were negatively regulated during epithelial cell proliferation. This indicated that RBMX2 can regulate cellular connectivity throughout the stages of M. bovis infection.

For KEGG analysis, genes linked to the MAPK signaling pathway, chemical carcinogen-DNA adducts, and chemical carcinogen-receptor activation were observed at 0 hpi. At 24 hpi, significant enrichment was found in the ECM-receptor interaction, PI3K-Akt signaling pathway, and focal adhesion. Upon enrichment analysis at 48 hpi, significant enrichment was noted in the TGF-beta signaling pathway, transcriptional misregulation in cancer, microRNAs in cancer, small cell lung cancer, and p53 signaling pathway.

> ***Reviewer #3 (Public review):***
>
> *Summary:*
>
> *This study investigates the role of the host protein RBMX2 in regulating the response to Mycobacterium bovis infection and its connection to epithelial-mesenchymal transition*

(EMT), a key pathway in cancer progression. Using bovine and human cell models, the authors have wisely shown that RBMX2 expression is upregulated following M. bovis infection and promotes bacterial adhesion, invasion, and survival by disrupting epithelial tight junctions via the p65/MMP-9 signaling pathway. They also demonstrate that RBMX2 facilitates EMT and is overexpressed in human lung cancers, suggesting a potential link between chronic infection and tumor progression. The study highlights RBMX2 as a novel host factor that could serve as a therapeutic target for both TB pathogenesis and infection-related cancer risk.

Strengths:

The major strengths lie in its multi-omics integration (transcriptomics, proteomics, metabolomics) to map RBMX2's impact on host pathways, combined with rigorous functional assays (knockout/knockdown, adhesion/invasion, barrier tests) that establish causality through the p65/MMP-9 axis. Validation across bovine and human cell models and in clinical tissue samples enhances translational relevance. Finally, identifying RBMX2 as a novel regulator linking mycobacterial infection to EMT and cancer progression opens exciting therapeutic avenues.

Weaknesses:

Although it's a solid study, there are a few weaknesses noted below.

(1) In the transcriptomics analysis, the authors performed (GO/KEGG) to explore biological functions. Did they perform the search locally or globally? If the search was performed with a global reference, then I would recommend doing a local search. That would give more relevant results. What is the logic behind highlighting some of the enriched pathways (in red), and how are they relevant to the current study?

We appreciate the reviewer's thoughtful questions regarding our transcriptomic analysis. In this study, we employed a localized enrichment approach focusing specifically on gene expression profiles from our bovine lung epithelial cell system. This cell-type-specific analysis provides more biologically relevant results than global database searches alone.

Regarding the highlighted pathways, these represent:

(1) Temporally significant pathways showing strongest enrichment at each stage:

- 0h: Cell junction organization (immediate barrier response)
- 24h: ECM-receptor interaction (early EMT initiation)
- 48h: TGF-β signaling (chronic remodeling)

(2) Mechanistically linked to our core findings about RBMX2's role in:

- Epithelial barrier disruption
- Mesenchymal transition
- Chronic infection outcomes

We selected these particular pathways because they:

(1) Showed the most statistically significant changes (FDR <0.001)

(2) Formed a coherent biological narrative across infection stages

(3) Were independently validated in our functional assays

This targeted approach allows us to focus on the most infection-relevant pathways while maintaining statistical rigor.

> *(2) While the authors show that RBMX2 expression correlates with EMT-related gene expression and barrier dysfunction, the evidence for direct association remains limited in this study. How does RBMX2 activate p65? Does it bind directly to p65 or modulate any upstream kinases? Could ChIP-seq or CLIP-seq provide further evidence for direct RNA or DNA targets of RBMX2 that drive EMT or NF-κB signaling?*

We sincerely appreciate the reviewer's in-depth questions regarding the mechanisms by which RBMX2 activates p65 and its association with EMT. Although the molecular mechanism remains to be fully elucidated, our study has provided experimental evidence supporting a direct regulatory relationship between RBMX2 and the p65 subunit of the NF-κB pathway. Specifically, we investigated whether the transcription factor p65 could directly bind to the promoter region of RBMX2 using CHIP experiments. The results demonstrated that the transcription factor p65 can physically bind to the RBMX2 region.

Furthermore, dual-luciferase reporter assays were conducted, showing that p65 significantly enhances the transcriptional activity of the RBMX2 promoter, indicating a direct regulatory effect of RBMX2 on p65 expression.

These findings support our hypothesis that RBMX2 activates the NF-κB signaling pathway through direct interaction with the p65 protein, thereby participating in the regulation of EMT progression and barrier function.

In our subsequent work papers, we will also employ experiments such as CLIP to further investigate the specific mechanisms through which RBMX2 exerts its regulatory functions.

> *(3) The manuscript suggests that RBMX2 enhances adhesion/invasion of several bacterial species (e.g., E. coli, Salmonella), not just M. bovis. This raises questions about the specificity of RBMX2's role in Mycobacterium-specific pathogenesis. Is RBMX2 a general epithelial barrier regulator or does it exhibit preferential effects in mycobacterial infection contexts? How does this generality affect its potential as a TB-specific therapeutic target?*

Thank you for your valuable comments. When we initially designed this experiment, we were interested in whether the RBMX2 knockout cell line could confer effective resistance not only against Mycobacterium bovis but also against Gram-negative and Gram-positive bacteria. Surprisingly, we indeed observed resistance to the invasion of these pathogens, albeit weaker compared to that against Mycobacterium bovis.

Nevertheless, we believe these findings merit publication in eLife. Moreover, RBMX2 knockout does not affect the phenotype of epithelial barrier disruption under normal conditions; its significant regulatory effect on barrier function is only evident upon infection with Mycobacterium bovis.

Importantly, during our genome-wide knockout library screening, RBMX2 was not identified in the screening models for Salmonella or Escherichia coli, but was consistently detected across multiple rounds of screening in the Mycobacterium bovis model.

> *(4) The quality of the figures is very poor. High-resolution images should be provided.*

Thank you for your feedback; we provided higher-resolution images.

> *(5) The methods are not very descriptive, particularly the omics section.*

Thank you for your comments; we have revised the description of the sequencing section.

> *(6) The manuscript is too dense, with extensive multi-omics data (transcriptomics, proteomics, metabolomics) but relatively little mechanistic integration. The authors should have focused on the key mechanistic pathways in the figures. Improving the narratives in the Results and Discussion section could help readers follow the logic of the experimental design and conclusions.*

Thank you for your valuable comments. We have streamlined the figures and revised the description of the results section accordingly.

https://doi.org/10.7554/eLife.107132.1.sa0